Mechanism of Tacrine Block at Adult Human Muscle Nicotinic Acetylcholine Receptors

Richard J. Prince,[1] Richard A. Pennington,[1] and Steven M. Sine[2]

[1]School of Biological Sciences, University of Manchester, Manchester M13 9PT, United Kingdom
[2]Department of Physiology and Biophysics, Mayo Clinic, Rochester, MN 55905

ABSTRACT We used single-channel kinetic analysis to study the inhibitory effects of tacrine on human adult nicotinic receptors (nAChRs) transiently expressed in HEK 293 cells. Single channel recording from cell-attached patches revealed concentration- and voltage-dependent decreases in mean channel open probability produced by tacrine (IC_{50} 4.6 μM at −70 mV, 1.6 μM at −150 mV). Two main effects of tacrine were apparent in the open- and closed-time distributions. First, the mean channel open time decreased with increasing tacrine concentration in a voltage-dependent manner, strongly suggesting that tacrine acts as an open-channel blocker. Second, tacrine produced a new class of closings whose duration increased with increasing tacrine concentration. Concentration dependence of closed-times is not predicted by sequential models of channel block, suggesting that tacrine blocks the nAChR by an unusual mechanism. To probe tacrine's mechanism of action we fitted a series of kinetic models to our data using maximum likelihood techniques. Models incorporating two tacrine binding sites in the open receptor channel gave dramatically improved fits to our data compared with the classic sequential model, which contains one site. Improved fits relative to the sequential model were also obtained with schemes incorporating a binding site in the closed channel, but only if it is assumed that the channel cannot gate with tacrine bound. Overall, the best description of our data was obtained with a model that combined two binding sites in the open channel with a single site in the closed state of the receptor.

KEY WORDS: kinetic analysis • open-channel block • single-channel recording • maximum likelihood • anticholinesterase

INTRODUCTION

The nicotinic acetylcholine receptor (nAChR)* from adult mammalian muscle is a heteropentameric protein with the subunit composition 2α, β, δ, ϵ. Each of the subunits is structurally homologous, and consists of a large, extracellular NH_2-terminal domain, four membrane spanning segments (M1-M4), and a large intracellular loop between M3 and M4. Contained within the nAChR complex are two binding sites for acetylcholine, which are located in the NH_2-terminal domains of the subunits, and a centrally located cation selective channel (Arias, 1996).

Although atomic structural insight recently emerged for the NH_2-terminal ligand binding domain via X-ray crystallography of an ACh binding protein (Brejc et al., 2001) and a mutagenesis-based model of the muscle receptor (Sine et al., 2002), our understanding of the transmembrane domains continues to rely on lower resolution cryoelectron microscopy studies (Miyazawa et al., 1999), site-directed mutagenesis, affinity labeling, and the substituted cysteine accessibility method (SCAM) (for review see Arias, 1996). Together, these techniques lead to a model of the receptor in which the subunits are arrayed around a central ion channel, with the lining of the channel formed largely by the M2 domains of each of the subunits, and perhaps, smaller contributions from the extracellular ends of the M1 segments. (Arias, 1996; Miyazawa et al., 1999)

The M2 domains are highly conserved amongst the subunits, meaning that the overall channel structure can be viewed as a series of rings, stacked one upon the other. Each ring consists of five homologous amino acids, one from each subunit. The secondary structure of these channel lining segments is thought to be α-helical but with a distinct "kink" part way along their length. At the apex of this kink in each subunit is a conserved leucine residue. In one current model of channel gating, the ring of bulky leucine residues projects into the channel and occludes ion flux when the channel complex is in the closed state. When agonists bind and the channel opens, the leucine residues swing out of the pore, allowing ions to pass (Unwin, 1995). An alternative model, derived from SCAM studies, holds that the

Address correspondence to Richard J. Prince, School of Biological Sciences, University of Manchester, Manchester M13 9PT, UK. Fax: (44) 161-275-5600; E-mail: richard.prince@man.ac.uk

*Abbreviations used in this paper: ACh, acetylcholine; AIC, asymptotic information criterion; DMEM, Dulbecco's modified Eagle's medium; HEK 293, human embryonic kidney 293; LL, log likelihood; LRT, likelihood ratio test; MIL, maximum interval likelihood; nAChR, nicotinic acetylcholine receptor; p.d.f, probability density function; SCAM, substituted cysteine accessibility method.

J. Gen. Physiol. © The Rockefeller University Press • 0022-1295/2002/09/369/25 $5.00
Volume 120 September 2002 369–393
http://www.jgp.org/cgi/doi/10.1085/jgp.20028583

channel gate is ~10 residues more cytoplasmic than the conserved leucine ring (Wilson and Karlin, 1998).

The ion channel of the nAChR is the target of a diverse group of noncompetitive antagonists that have generally been classified as open channel blockers (for review see Arias, 1996). Open channel blockers inhibit receptor function by entering and physically plugging the open channel, thereby preventing ion flux. Because the binding site is accessible only when the channel has been activated, and is located within the membrane field, the actions of open channel blockers are use and voltage dependent. Photoactivatible open channel blockers (e.g., chlorpromazine) were instrumental in pinpointing residues that line the channel and hence in the identification of the M2 segments as the major structural components of the channel (Changeux, 1990; Arias, 1996). However, despite the historical importance of open channel blockers in structure–function studies, our knowledge of their sites and mechanisms of action is incomplete. In particular, there have been very few systematic investigations of the kinetics of open channel block at the single channel level.

In this study, we investigated the blocking mechanism of tacrine (9-amino-1,2,3,4-tetrahydroacridine) at human adult nAChRs. Tacrine is used clinically to treat Alzheimer's disease and is thought to exert its therapeutic effects via inhibition of acetylcholinesterase. However, at higher concentrations than those used in the clinic, tacrine has also been found to inhibit a wide range of other proteins, including K^+ channels (Dreixler et al., 2000), NMDA receptors (Hershkowitz and Rogawski, 1991; Vorobjev and Sharonova, 1994), voltage-gated Ca^{2+} channels (Dolezal et al., 1997), and muscarinic acetylcholine receptors (Perry et al., 1988; Kiefer-Day et al., 1991; Kojima and Onodera, 1998). Previous studies showed that tacrine is a noncompetitive antagonist of *Torpedo* electric organ nAChRs (Canti et al., 1998), and speculated that the mechanism of this inhibition may involve open channel block. In the present study, we used maximum likelihood techniques to fit a series of kinetic models to single channel data. Our results suggest that tacrine is an atypical open channel blocker and interacts with at least two sites within the open- and one in the closed-state of the receptor. Thus, there may be multiple binding sites for tacrine and structurally related compounds in the nAChR complex.

MATERIALS AND METHODS

Materials

Dulbecco's modified Eagle's medium (DMEM), penicillin, and streptomycin were purchased from GIBCO BRL. Tacrine was purchased from RBI. All other materials were obtained from Sigma-Aldrich. [^{125}I]-labeled α-bungarotoxin was obtained from Amersham Biosciences. The sources of the human nAChR subunits were as described previously (Ohno et al., 1996).

Cell Culture and Receptor Expression

Human embryonic kidney 293 (HEK 293) cells were maintained in culture at 37°C, 5% CO_2 in DMEM containing 10% FCS, 50 IU/ml penicillin, and 50 μg/ml streptomycin. In all experiments, cells were transfected at ~30% confluency using calcium phosphate precipitation as previously described (Prince and Sine, 1996). For each 35-mm culture dish, 2.7 μg of α subunit DNA and 1.35 μg each of β, δ, and ϵ were used in the transfection mixture. A plasmid encoding fluorescent green protein (pGreen lantern) was also included (0.5 μg/35 mm plate) in the transfection mixture to allow identification of transfected cells under fluorescence optics. The culture medium was replaced with fresh medium 12–16 h after transfection, and the cells were maintained at 37°C for a further 24–48 h before recordings or binding studies were performed.

Patch-clamp Recording

Recordings were obtained from transfected HEK 293 cells in the cell-attached configuration at membrane potentials of −70, −110 or −150 mV, at a temperature of 23°C. The bath and pipette solutions contained KRH buffer: (in mM) KCl 142, NaCl 5.4, $CaCl_2$ 1.8, $MgCl_2$ 1.7, and HEPES 25, pH 7.4. The patch pipette also contained various concentrations of acetylcholine (ACh) and tacrine, as required.

Recordings were made using an Axopatch 200A amplifier at a bandwidth of 50 kHz. Data were digitized at 200 kHz using an ITC-16 analogue to digital interface and recorded directly to hard-disk using the program Acquire (Bruxton Instruments). Channel openings and closings were detected off-line by the half-amplitude criterion using the program TAC (Bruxton Instruments) at a final bandwidth of 10 kHz. Open- and closed-duration histograms of the idealized data were constructed using TACFit (Bruxton Instruments) and were fitted by the sums of exponential functions.

At the concentrations of ACh (6–300 μM) used in this study, channel openings group into clusters corresponding to activation episodes of single AChRs. The long closings that mark the boundaries of clusters correspond to periods when all channels in the patch are in a desensitized conformation. Data within clusters were identified and selected for maximum likelihood analysis as described previously (Prince and Sine, 1998a). For each recording, we calculated the mean open and closed durations within clusters (m_{open}, m_{closed}) and the mean probability that the channel was open within clusters of openings (P_{open}). Concentration-response curves for ACh were constructed using P_{open} values and were fitted using the following form of the Hill equation:

$$P_{open} = \frac{M.X^n}{X^n + EC_{50}^n}, \quad (1)$$

where X represents the concentration of ACh, M is the fitted maximum P_{open}, EC_{50} is the concentration of ACh yielding 50% of maximal P_{open}, and n is the Hill coefficient.

Tacrine inhibition curves were fitted using the following equation:

$$P_{open} = M.\left(1 - \frac{X^n}{X^n + IC_{50}^n}\right), \quad (2)$$

where X represents the concentration of tacrine, M is the P_{open} in the absence of tacrine, IC_{50} is the concentration of tacrine that yields a P_{open} of 50% of M, and n is the Hill coefficient.

Maximum Likelihood Analysis

To determine the rate constants governing receptor activation and block by ACh, recordings obtained over a range of ACh con-

centrations (6–300 μM) were analyzed according to Scheme A (see Fig. 3) using the maximum interval likelihood (MIL) program developed by Qin et al. (1996). A dead-time of 22 μs was imposed on all recordings. The MIL program calculates the likelihood that a given kinetic scheme and set of rate constants gave rise to the experimental set of openings and closings. The program then systematically varies the rate constants to maximize the likelihood. Once the parameters in Scheme A had been established, recordings obtained with 100 μM ACh and 1–60 μM tacrine (data at 60 μM tacrine were included only at −70 mV) were analyzed according to mechanisms B-I (see Fig. 3), with the values of the parameters for activation and block of the receptor by ACh constrained to the values determined by fits to Scheme A in the absence of tacrine (see Table IV). Nested models (models derived from the same parent kinetic scheme) were compared using the likelihood ratio test (LRT) statistic (Rao, 1973):

$$LRT = 2.(LL_1 - LL_2),$$

where LL_1 and LL_2 are the log-likelihood values of the models being compared. LRT is distributed as χ^2 with the degrees of freedom being the difference in the number of free parameters between the two models.

We also made a global comparison of all models using the asymptotic information criterion (AIC) (Akaike, 1974). The AIC provides a method of comparing nonnested models and is calculated thus:

$$AIC = 2.(n - LL),$$

where n is the number of free parameters and LL is the log-likelihood value for the model under consideration. The model with the minimum AIC value is considered the best.

Ligand Binding Assays

48 h after transfection, the growth medium was removed and the HEK 293 cells were harvested by gentle agitation in phosphate-buffered saline containing 5 mM EDTA. The cells were centrifuged for 5 min at 1500 *g* and then resuspended in KRH buffer containing 30 mg/l BSA. Tacrine affinity was determined by competition against the initial rate of [^{125}I]-labeled α-bungarotoxin binding (Prince and Sine, 1998b). In a separate set of experiments designed to test the possibility that tacrine could desensitize the receptor, cells were preincubated for 1 h with the required concentrations of tacrine and carbamylcholine before addition of [^{125}I]-labeled α-bungarotoxin.

Nonspecific binding was determined in the presence of 10 mM carbamylcholine. Binding data were analyzed according to the following form of the Hill equation:

$$1 - f_{occ} = 1 - \frac{X^n}{X^n + IC_{50}^n}, \quad (3)$$

where f_{occ} is the fractional occupancy of receptor by the competing ligand, X is the concentration of competing ligand, n is the Hill coefficient, and IC_{50} is the concentration of the competing ligand that yields 50% occupancy of the receptor. Nonlinear regression was performed using Prism 3.0 (GraphPad Software).

RESULTS

Ligand Binding Experiments

To assess whether tacrine competes with ACh at the receptor agonist binding sites, we determined the affinity of tacrine by competition against the initial rate of [^{125}I]-labeled α-bungarotoxin binding. Tacrine bound with an IC_{50} of 309 ± 30 μM and a Hill coefficient of 1 ± 0.1 (n = 3) (Fig. 1 A). As described below, ACh-induced currents are antagonized by much lower concentrations of tacrine, eliminating competitive antagonism as the primary mechanism for functional inhibition of the nAChR by tacrine.

In a separate series of binding experiments, we assessed whether tacrine could desensitize the nAChR by determining the affinity of carbamylcholine in the presence of varying concentrations of tacrine (Fig. 1 B). No difference was seen in log IC_{50} values for carbamylcholine (P = 0.64 by one-way ANOVA), indicating that tacrine does not produce the increase in ACh affinity expected of a desensitizing agent (Sine and Taylor, 1982).

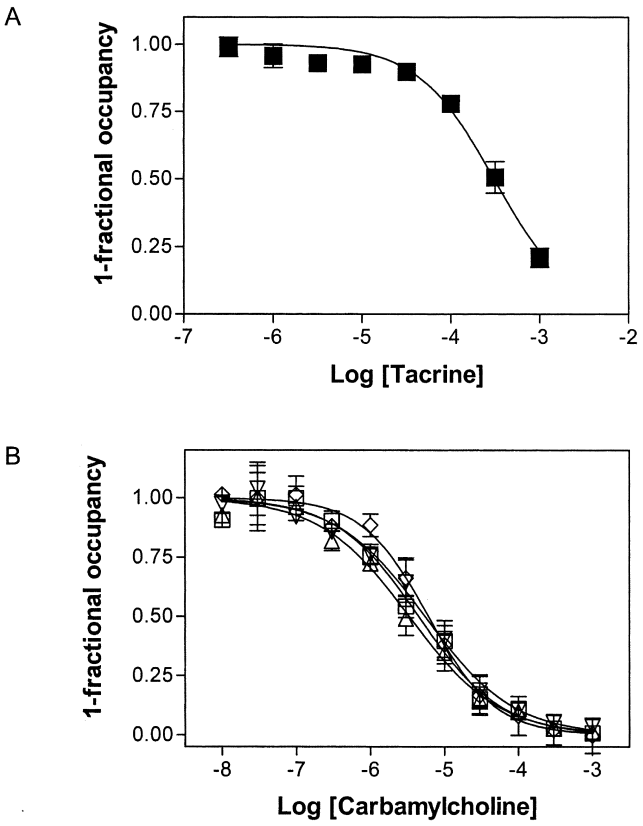

FIGURE 1. (A) Steady-state binding of tacrine to nAChRs. The smooth curve is a fit of the Hill equation (Eq. 3) to the data with the following parameters IC_{50} = 309 ± 30 μM, n = 1 ± 0.1. (B) Steady-state binding of ACh to nAChRs in the presence of 0, 1, 10, 100 μM tacrine. Fits of the Hill equation to the data yielded the following parameters: 0 tacrine (□) IC_{50} = 4.5 ± 0.7 μM, n = 0.8 ± 0.1; 1 μM tacrine (△) IC_{50} = 3.4 ± 0.4, n = 0.7 ± 0.1; 10 μM tacrine (▽) IC_{50} = 5.5 ± 0.7 μM, n = 0.7 ± 0.1; 100 μM tacrine (◇) IC_{50} = 6.1 ± 1 μM, n = 1 ± 0.1. For both types of experiment, ligand affinity was determined by competition against the initial rate of [^{125}I]-labeled α-bungarotoxin as described in MATERIALS AND METHODS. Each point is the mean of three determinations and the error bars represent the SEM.

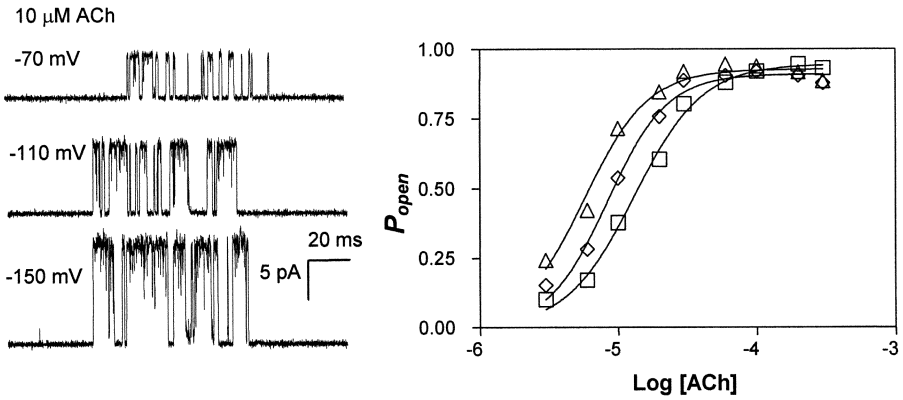

FIGURE 2. Activation of human adult muscle nicotinic acetylcholine receptors by ACh. (Left) Openings of single receptors were grouped into clusters bounded by long closings. (Right) Concentration-response curves for adult human nAChRs activated by ACh (□, −70 mV; ◇, −110 mV; △, −150 mV). The overall P_{open} for each recording was calculated at the indicated concentrations as described in MATERIALS AND METHODS. The data are the mean of 2–5 recordings and the solid lines are fits to the Hill equation (Eq. 1). Parameters for these fits are given in Table I.

Patch-Clamp Experiments: Initial Observations

Activation by ACh. We recorded responses to 6–300 μM ACh at three membrane potentials: −70, −110, and −150 mV. At each potential, periods of channel activity corresponding to the activation of single nAChRs were readily discernible as clusters of channel openings bounded by long closed times (Fig. 2). For each recording, we calculated the mean P_{open} (probability that the channel is in the open state) within clusters and fitted the Hill equation to our data. The resulting concentration-response curves revealed Hill coefficients close to two at each potential and a voltage-dependent decrease in EC_{50} (Fig. 2, Table I).

Within clusters, there were two main components in the closed time histogram. The faster component (∼20 μs) did not vary in duration, but increased in relative area with increased ACh concentration. In contrast, the longer component of intracluster closings (∼100 μs at 100 μM ACh) decreased in relative area with tacrine concentration but moved progressively to shorter durations. This component of the closed time histogram is described by a rate constant termed β′, (also known as effective channel opening rate) (Sine and Steinbach, 1987) and arises from dwells of the channel in the C, AC, and A_2C states (Fig. 3, Scheme A).

The long closed times which bound clusters of openings are thought to represent periods when all receptors in the patch are desensitized. We observed three exponential components of desensitization closed times in this study. Long (∼7.5 s) duration closings were observed at all concentrations of ACh and were somewhat variable in duration. desensitization on this time scale has been reported in numerous studies dating back to Katz and Thesleff (1957). Medium (∼30 ms) duration desensitization closings could be resolved at concentrations above 10 μM ACh, but were obscured by slower components of the closed time probability density function (p.d.f.) at lower concentrations of agonist. This type of desensitization was of constant duration across the concentration range 20–300 μM and is in good agreement with results from rapid agonist application experiments which have yielded desensitization time constants of 15–50 ms (Dilger and Liu, 1992; Franke et al., 1992; Jahn et al., 2001). A similar duration closed-time component was also observed by Sine and Steinbach (1987) in single channel recordings from BC3H-1 cells. Finally, at concentrations of 60 μM ACh and above we observed a fast (2 ms) desensitization component that did not alter in duration with agonist concentration. A similar (4.5 ms) component was noted by Zhang et al. (1995) and was assumed to represent a rapid form of desensitization.

TABLE I

Activation of Adult Human nAChRs by Acetylcholine

Membrane potential	EC_{50}	n	M
mV	*μM*		
−70	13.2 ± 0.46	1.8 ± 0.09	0.95 ± 0.01
−110	8.43 ± 0.34	2.01 ± 0.16	0.91 ± 0.01
−150	5.74 ± 0.33	1.88 ± 0.19	0.93 ± 0.02

The parameters and error estimates are derived from fits of the Hill equation (Eq. 1) to the data shown in Fig. 1. Each fitted parameter is expressed ± SE. EC_{50} is the concentration which yields 50% of the maximal response, n is the Hill coefficient, and M is the fitted maximum P_{open}.

Inhibition by tacrine. To determine the effects of tacrine on ACh-evoked single channel activity, we recorded responses to 100 μM ACh in the presence of 1–100 μM tacrine at membrane potentials of −70, −110 and −150 mV. We chose 100 μM ACh because it allowed clusters to be identified over a wide range of tacrine concentrations. Inclusion of tacrine in the patch pipette produced a concentration- and voltage-dependent reduction in channel open probability with fitted IC_{50} values close to 3 μM (Fig. 4, Table II). In a separate series of experiments, we recorded responses to 300 μM ACh in the presence of 10 μM tacrine. As predicted for noncompetitive antagonism, the reduction in P_{open} (expressed as percentage change from control) produced by 10 μM tacrine at 300 μM ACh (74%)

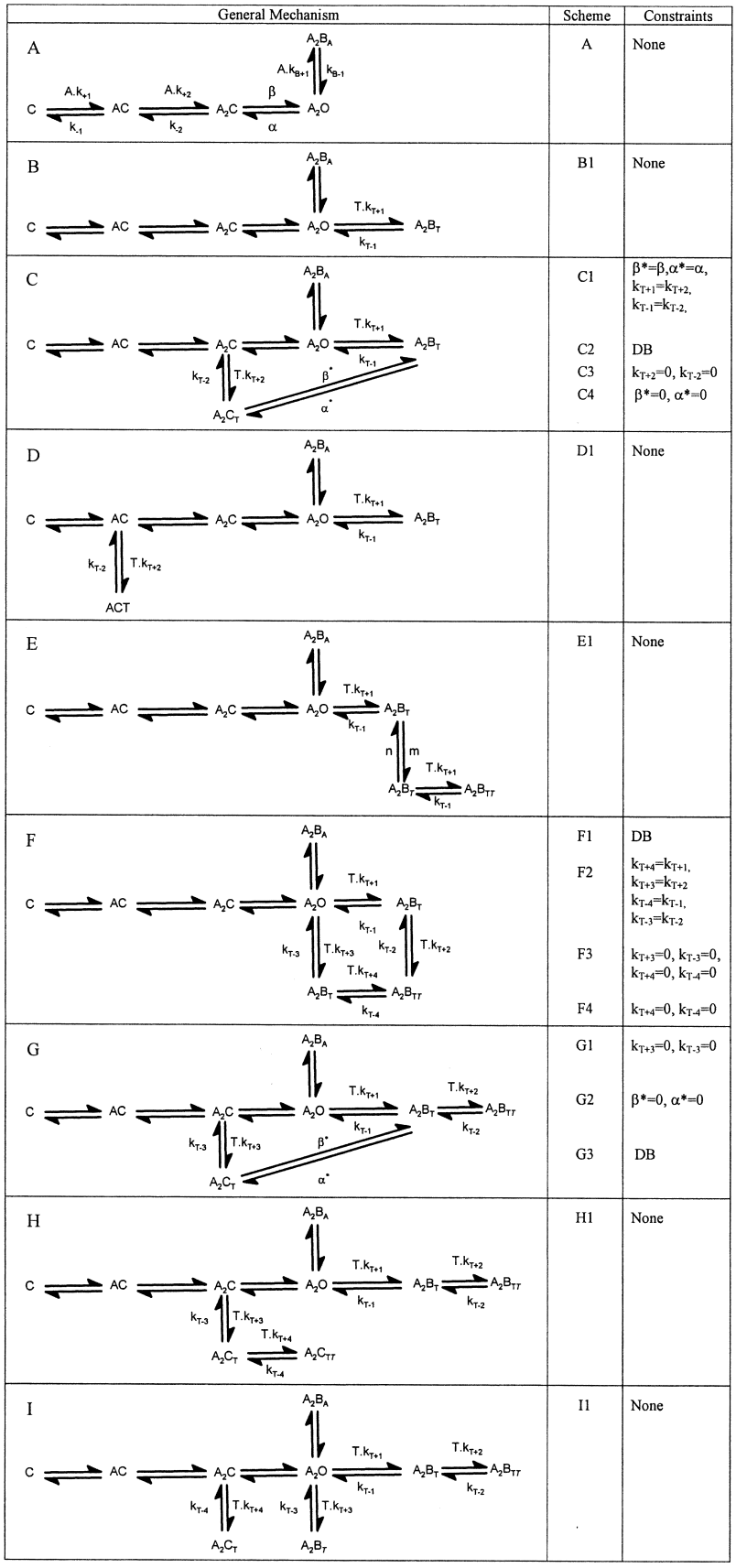

FIGURE 3. Kinetic schemes used in maximum likelihood fitting. (Notation used for receptor states) C, AC, A_2C are closed states with agonist binding sites unoccupied, singly occupied, and doubly occupied, respectively; A_2O is the open state; A_2B_A is the open state blocked by acetylcholine; A_2B_T and A_2B_T are distinct open-blocked states that have bound tacrine to one site within the channel; A_2B_{TT} is an open blocked state in which tacrine has bound to two sites within the channel; A_2C_T and A_2C_{TT} are closed states which have bound one and two molecules of tacrine respectively. (Notation used for rate constants) General mechanism. (A) β, α are channel opening and closing rate constants respectively; k_{+1}, k_{+2}, k_{B+1} are association rate constants for ACh at the two agonist binding sites and channel block site respectively; k_{-1}, k_{-2}, k_{B-1} are dissociation rate constants for ACh at the two agonist binding sites and channel block site, respectively. A is the concentration of ACh. General mechanisms B–I: k_{T+1}, k_{T+2}, k_{T+3} and k_{T+4} are association rate constants for tacrine and k_{T-1}, k_{T-2}, k_{T-3} and k_{T-4} are dissociation rate constants; β* and α* are channel opening and closing rate constants with tacrine bound; m and n are the forward and backward rate constants for the diffusion of tacrine between a shallow site within the channel to a deeper site; T is the concentration of tacrine. DB indicates that the scheme was constrained by detailed balancing. In general mechanisms B–I, only the rate constants that were derived by maximum likelihood fitting are shown. Other rate constants within the schemes were fixed to values determined from fitting to Scheme A (see Table IV).

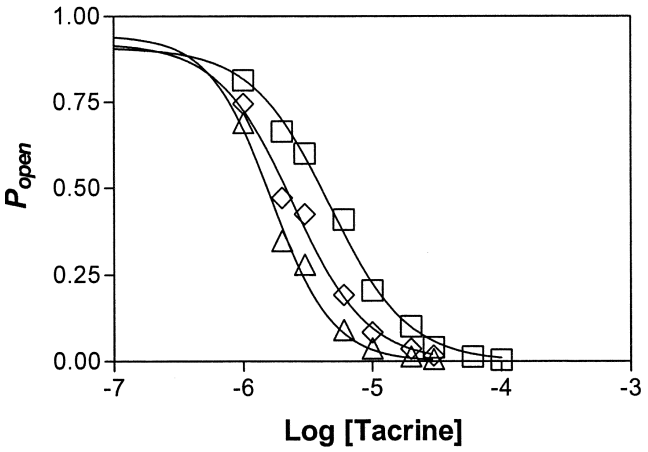

FIGURE 4. Tacrine inhibition of responses to 100 μM ACh at −70 mV (□), −110 mV (◇), and −150 mV (△) membrane potential. The data are the mean of 2–4 recordings and the solid lines are fits to the Hill equation (Eq. 2). The parameters derived from these fits are summarized in Table II. The top of each curve was fixed to the mean P_{open} obtained in the absence of tacrine.

was essentially the same as that produced at 100 μM ACh (77%). To determine whether tacrine can act as an agonist at the nAChR we made recordings with 10 μM tacrine and no ACh in the patch pipette. No responses were observed in the presence of tacrine alone ($n = 3$).

Effects of Tacrine on Dwell-time Distributions

Preliminary examination of channel open- and closed-times revealed that tacrine decreased m_{open} and increased m_{closed}. These effects are strongly suggestive of open channel block, which for the nAChR has been described classically by Scheme B1 (Fig. 3).

In Scheme B1 (Neher and Steinbach, 1978), the open-blocked state (A_2B_T) is connected only to the open state (A_2O). This simple connectivity means that the rate constants k_{T+1} and k_{T-1} can be determined by examining the effects of blocker on the distributions of open, burst, and closed durations. As in most previous studies of nAChR channel block, therefore, Scheme B1 was our starting point from which to investigate the kinetics of block.

TABLE II

Inhibition of Adult Human nAChRs by Tacrine

Membrane potential	IC_{50}	n
mV	*μM*	
−70	4.6 ± 0.23	1.4 ± 0.08
−110	2.5 ± 0.24	1.5 ± 0.15
−150	1.6 ± 0.09	1.9 ± 0.19

The parameters and error estimates are derived from fits of Eq. 2 to the data shown in Fig. 2. Each fitted parameter is expressed ± SE. IC_{50} is the concentration of tacrine that produces a 50% reduction in P_{open}. n is the Hill coefficient.

Open Time Distributions

More-detailed examination of the open-duration histograms (Fig. 5 A) revealed that the tacrine-induced decrease in mean channel open time was concentration and voltage dependent. Neglecting for the moment block of the channel by ACh itself, Scheme B1 predicts the reciprocal of the mean channel open duration (τ_{open}) to be related linearly to the concentration of open channel blocker (T):

$$\frac{1}{\tau_{open}} = \alpha + T.k_{T+1}. \quad (4)$$

To apply Eq. 4 to experimental data, it is first necessary to correct apparent mean open durations for unresolved dwells in the closed states. These missed closings result in the concatenation of successive channel openings and thus in an overestimation of τ_{open}. In the present study, the exact form of Eq. 4 cannot be used because the partially resolved brief closings that arise from channel gating are of a similar duration to those that arise from block of the channel by ACh itself. However, it can be demonstrated (APPENDIX A) that open time correction can be omitted for our present data and that using the apparent mean open time (τ_{app}), yields a straight-line with a slope approximating k_{T+1}:

$$\frac{1}{\tau_{app}} = \frac{1}{\tau_0} + T.k_{T+1}, \quad (5)$$

where τ_0 is the apparent mean open time at zero tacrine concentration. Plots of Eq. 5 are shown in Fig. 5 B.

Burst-duration Distributions

An alternative method of investigating channel block is the integration method of Neher (1983). The integration method makes use of the fact that for sequential block, burst duration increases with blocker concentration, but the total open time per burst does not vary. On the other hand, "parallel block" models such as Scheme C2 (Fig. 3) that provide the receptor with a pathway back to the closed state, thereby bypassing the unblocked open state, predict a decrease in the total open time per burst. Therefore, in theory, the integration method can distinguish between sequential and parallel block mechanisms. However, a limitation of the integration method is that it can only be used when individual bursts can be identified unequivocally, i.e., at low concentrations of agonist where the mean duration of block closings is shorter than $1/\beta'$. In the present study, this condition cannot be met because even at the lowest concentrations of tacrine, the mean block duration is considerably longer than $1/\beta'$.

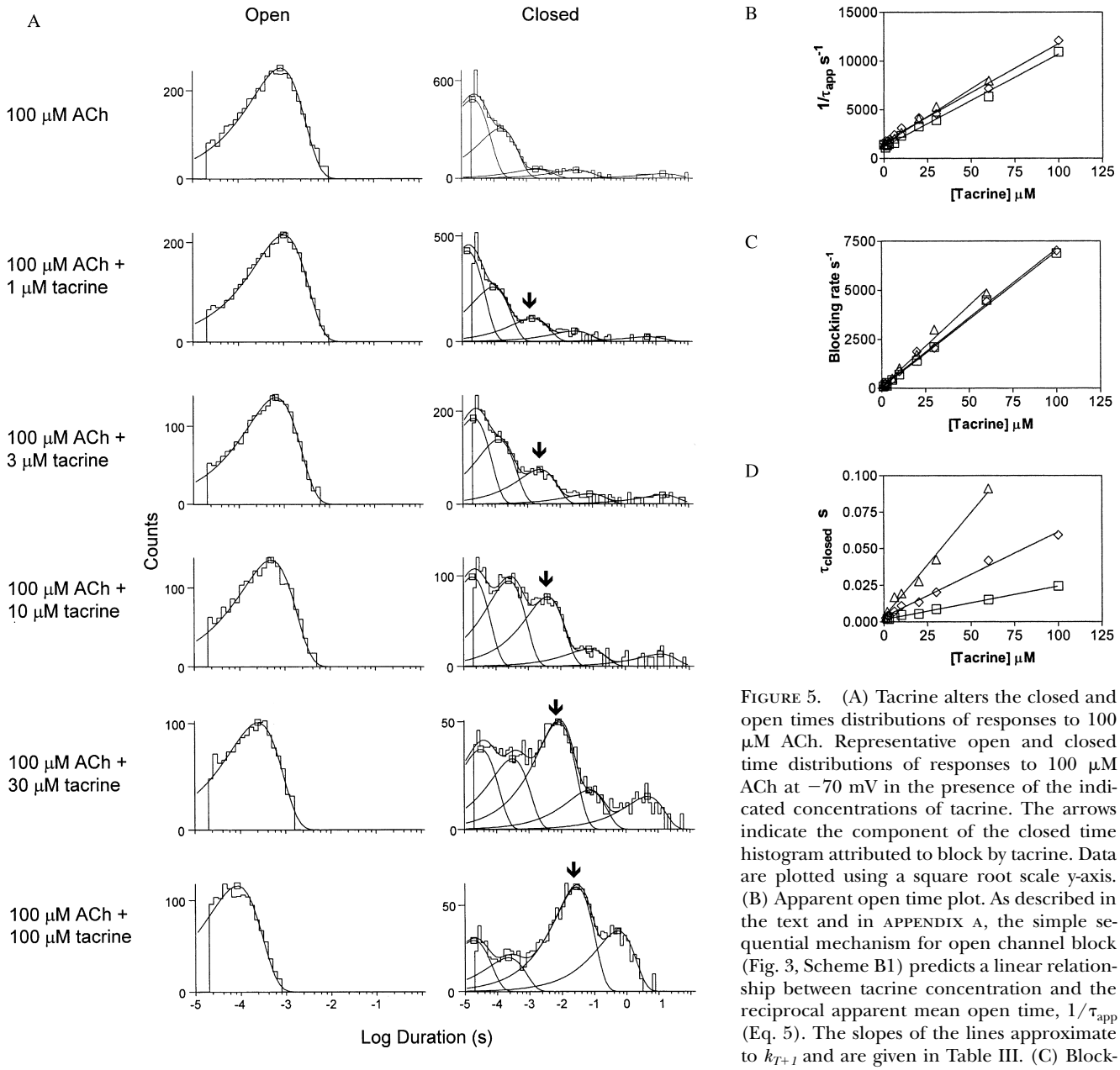

FIGURE 5. (A) Tacrine alters the closed and open times distributions of responses to 100 μM ACh. Representative open and closed time distributions of responses to 100 μM ACh at −70 mV in the presence of the indicated concentrations of tacrine. The arrows indicate the component of the closed time histogram attributed to block by tacrine. Data are plotted using a square root scale y-axis. (B) Apparent open time plot. As described in the text and in APPENDIX A, the simple sequential mechanism for open channel block (Fig. 3, Scheme B1) predicts a linear relationship between tacrine concentration and the reciprocal apparent mean open time, $1/\tau_{app}$ (Eq. 5). The slopes of the lines approximate to k_{T+1} and are given in Table III. (C) Blocking frequency plot. Blocking frequency is the number of blocking events per unit time and was calculated as described in the text (Eq. 6). Scheme B1 (Fig. 3) predicts a straight-line relationship between blocking frequency and tacrine concentration. The slopes of the lines are predicted to be equal to k_{T+1} and are given in Table III. (D) Mean durations of channel closings arising from block by tacrine. The symbols used in B, C, and D are as follows: −70 mV (□), −110 mV (◇), and −150 mV (△).

Closed-time Distribution

Predictions about the closed time distribution can also be made from Scheme B1. First, open channel block should produce a new class of closings and these closings should increase in frequency with increasing blocker concentration. Ogden and Colquhoun (1985) exploited this predicted increase in "blocking frequency" to calculate blocker association rate constants. Blocking frequency (B_f) is simply the number of blocking events per unit time and is calculated thus:

$$B_f = \frac{N_{block}}{N_{open} \cdot m_{open}}, \quad (6)$$

where N_{block} is the number of closings attributable to block by tacrine, N_{open} is the number of channel openings (corrected for missed openings), and m_{open} is the apparent mean channel open time. For blockers that follow Scheme B1, plots of B_f against blocker concentration should be straight lines with slopes of k_{T+1}. As predicted by Scheme B1, tacrine produced an additional exponential component in the closed time distri-

TABLE III

Fit Parameters for Apparent Open Time and Blocking Frequency Plots

	Membrane potential		
	−70	−110	−150
	mV	*mV*	*mV*
Apparent open time plot			
k_{T+1} ($\mu M^{-1}\ s^{-1}$)	95 ± 2	100 ± 3	114 ± 5
Intercept (s^{-1})	1,195 ± 86	1,744 ± 101	1,456 ± 112
Blocking frequency plot			
k_{T+1} ($\mu M^{-1}\ s^{-1}$)	69 ± 1	70 ± 4	83 ± 5
Intercept (s^{-1})	37 ± 47	97 ± 143	76 ± 138

Fit parameters are from linear regression to the data in Fig. 5, B and C, and are given ± SE (errors derived from linear regression). According to Scheme B1, the slope of either plot should give an estimate of the association rate for tacrine (k_{T+1}). At each membrane potential, comparison of the slopes (Zar, 1984) revealed that the two plot methods yield significantly different values of k_{T+1} ($P < 0.0005$).

TABLE IV

Kinetic Parameters for ACh Activation of Human Adult nAChRs

	−70 mV	−110 mV	−150 mV
k_{+1}	211 ± 11	140 ± 9	138 ± 15
k_{-1}	4,126 ± 260	2,654 ± 248	1,845 ± 228
K_1	19.6	19	13.4
k_{+2}	165 ± 4	148 ± 5	139 ± 5
k_{-2}	20,261 ± 262	13,410 ± 231	10,345 ± 226
K_2	123	90.6	74.4
β	53,211 ± 1,163	54,585 ± 1,254	57,352 ± 1591
α	2,290 ± 49	1,770 ± 46	1,373 ± 48
Θ	23.2	30.8	41.8
k_{+b}	38 ± 4	77 ± 3	90 ± 3.2
k_{-b}	149,000 ± 4,122	97,761 ± 2,004	105,963 ± 1,671
K_B	3,921	1,270	1,177

Parameters were derived from maximum likelihood fitting of Scheme A (Fig. 3) to single-channel data obtained at ACh concentrations from 6–300 mM and are expressed ± SE. The rate constants are defined in the legend to Fig. 3. Association rate constants are given in units of $\mu M^{-1}\ s^{-1}$, and all others in units of s^{-1}. K_1, K_2 and K_B (mM) are dissociation constants governing the binding of ACh to the high- and low-affinity agonist binding sites and the channel block site, respectively. Θ is the equilibrium constant governing channel opening. K_1, K_2, K_B, and Θ were calculated from their constituent rate constants.

bution, the relative area of which increased with tacrine concentration (Fig. 5 A). Blocking frequency plots for tacrine derived using this component (Fig. 5 C) were straight lines and yielded values of k_{T+1} close to, but consistently smaller than, those derived from Eq. 5 (Table III). As discussed below, these differences are predicted by our kinetic modelling studies.

A final prediction of Scheme B1 is that the time constant of block closings should depend solely on the dissociation constant of the blocker (k_{T-1}) and thus should be concentration independent. Contrary to Scheme B1, however, the duration of block closings increased with increasing tacrine concentration (Fig. 5, A and D).

Taking our initial analyses of open and closed distributions together, our data strongly suggest that tacrine inhibits the nAChR by interacting with the open channel but the mechanism of this inhibition is incompatible with Scheme B1. To gain further insight into how tacrine interacts with the nAChR we therefore decided to fit a series of kinetic models to our single channel data using maximum likelihood techniques.

Maximum Likelihood Analysis

Kinetics of activation of the receptor by ACh. Detailed kinetic analysis of the mechanism by which tacrine inhibits the nAChR requires knowledge of the rate constants that govern activation of the receptor by ACh in the absence of tacrine. To estimate these rate constants we recorded currents at 6–300 μM ACh and analyzed the resulting open and closed dwell times using maximum likelihood fitting (MATERIALS AND METHODS). We used a standard linear scheme (Fig. 3, Scheme A) to describe activation of the receptor and block by ACh itself. Scheme A does not include monoliganded openings of the receptor, but at the concentrations of ACh used in this series of experiments only a single class of openings was observed. Scheme A should therefore be a good approximation of reality under the conditions used in this study. A global set of rate constants (Table IV) for Scheme A was obtained by simultaneous fitting to data obtained over the range of ACh concentrations, and the resulting probability density functions are shown as smooth curves superimposed on the open and closed time histograms (Fig. 6). The rate constants derived from this series of experiments are, at −70 mV, very similar to those observed by Ohno et al. (1996). Our results reveal that the voltage dependence of the EC_{50} of ACh is largely due to decreases in the channel closing rate (α) and the rates of dissociation of ACh from the agonist binding sites (k_{-1}, k_{-2}).

Kinetics of tacrine inhibition. Once the parameters for channel activation by ACh were determined, we applied maximum likelihood fitting techniques to recordings made at 100 μM ACh in the presence of tacrine. We fitted 16 schemes to our data (Fig. 3), constraining the rate constants for activation and block of the nAChR by ACh to the values in Table IV. Global fitting was again performed by simultaneous fitting of data obtained over a range of tacrine concentrations.

First, we considered the classic sequential scheme for open channel block (Scheme B1). A priori, Scheme B1 cannot account for the inhibition of the nAChR by tacrine because it predicts that the durations of block closings should be independent of tacrine concentration. However, fitting Scheme B1 to our data provides a baseline for comparing the merits of other models. As expected, Scheme B1 yielded a poor fit to our data, particularly in the closed time distribution.

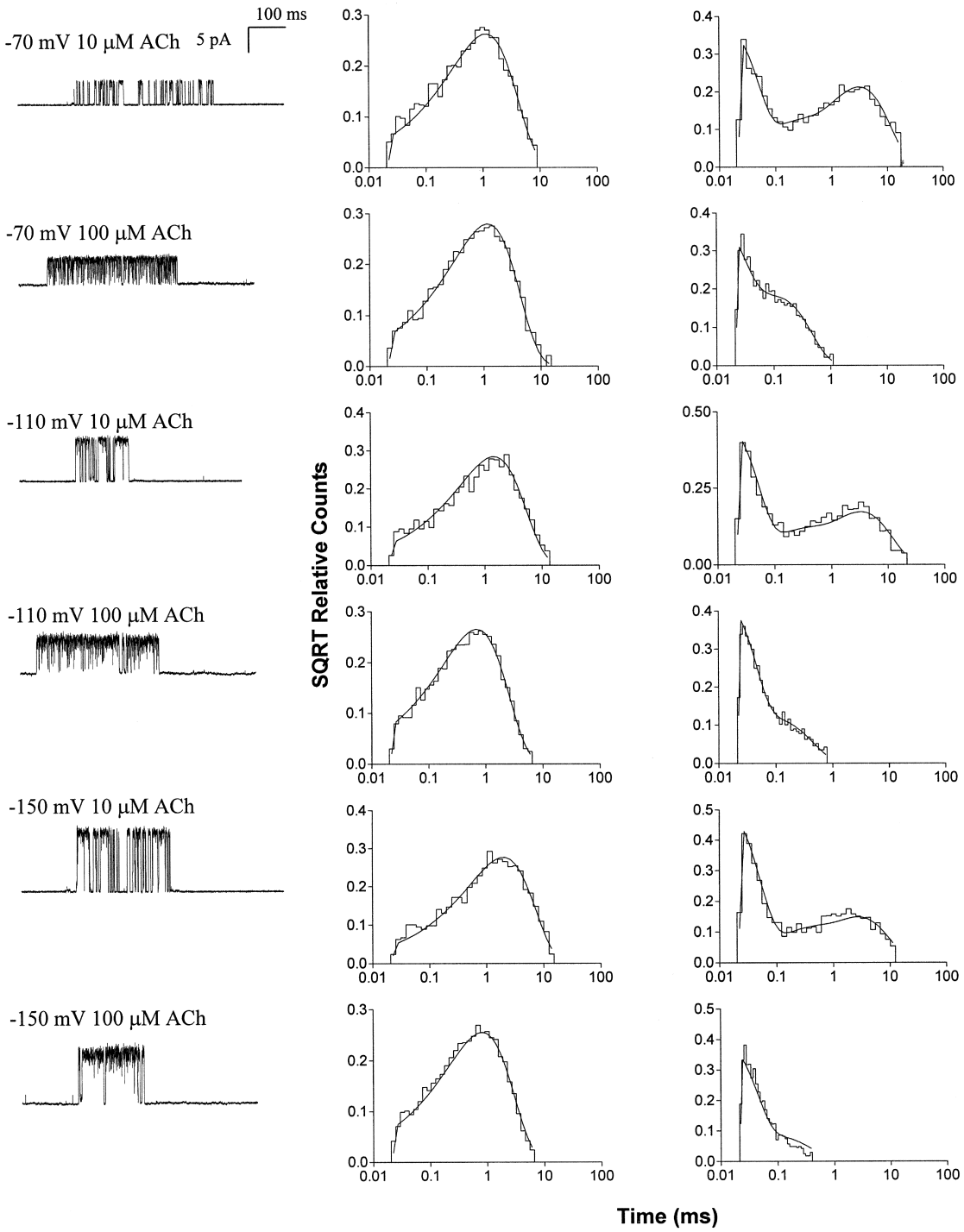

FIGURE 6. Kinetics of activation of nAChRs by acetylcholine. Left panels show traces of individual clusters from patches recorded at the indicated concentrations of ACh. The traces are displayed at a bandwidth of 5 kHz. The smooth curves through the open and closed time histograms are theoretical probability density functions calculated from the fitted rate constants for Scheme A (Fig. 3), with values given in Table IV. At least two recordings were obtained at each of the following concentrations of ACh: 6, 10, 20, 30, 60, 100, 200, 300 μM. For each concentration, the number of clusters selected for analysis ranged from 85–198 (−70 mV), 49–111 (−110 mV) and 43–135 (−150 mV), while the number of events ranged from 7,330–11,190 (−70 mV), 7,686–14,080 (−110 mV) and 4,658–15,638 (−150 mV).

Next, we fitted a series of kinetic schemes to our data that described more complex interactions between tacrine and the receptor (Fig. 3). We considered three general mechanisms by which tacrine might bind to and inhibit the function of the nAChR: (a) competitive inhibition at the nAChR agonist binding sites; (b) binding to the closed channel; and (c) binding to the open channel. The individual schemes

TABLE V

Comparisons of Log-likelihood and AIC Values for Schemes B1–I1

Scheme	−70 mV		−110 mV		−150 mV	
	LL	AIC	LL	AIC	LL	AIC
B1	398,409	15	461,905	15	260,617	15
C1	398,362	16	461,871	16	260,606	16
C2	399,441	12	462,675	12	261,402	12
C3	399,441	11	462,675	11	261,402	11
C4	399,061	13	462,477	13	261,307	13
D1	398,633	14	461,958	14	260,874	14
E1	400,796	10	463,522	10	262,221	10
F1	401,027	6	463,642	2	262,310	3
F2	400,846	9	463,569	9	262,253	9
F3	401,018	8	463,635	7	262,287	8
F4	401,027	5	463,642	1	262,310	2
G1	401,024	7	463,641	2	262,292	7
G2	401,037	1	463,638	6	262,306	4
G3	401,036	4	463,641	5	262,306	5
H1	401,038	3	463,638	8	262,306	6
I1	401,039	1	463,643	2	262,314	1

Log-likelihood (LL) values were generated by maximum likelihood fitting using the program MIL (Qin et al., 1996). AIC ranks were assigned as described in the text.

are described in detail in the DISCUSSION. However, the following general observations can be made by considering AIC ranking (Table V): (a) schemes that allowed tacrine to bind within the closed channel of the receptor produced an improved fit relative to the sequential scheme, but only if it was assumed that the channel could not open or close with tacrine bound (Schemes C4, G2); (b) improvements relative to the sequential model were also obtained with models that allowed tacrine to bind only to the open channel but also allowed the channel to close with tacrine still bound (Schemes C3, G1); (c) schemes that postulated two binding sites for tacrine within the open channel of the receptor (Mechanisms E–I) yielded dramatic improvements in goodness of fit; (d) the best schemes had two binding sites in the open state and allowed interactions between tacrine and the closed state (Mechanisms G–I). Taking into account our results from maximum likelihood analysis and from single channel simulations (see below), the best overall description of our data is achieved with Scheme G2. Fig. 7 shows the predicted probability density functions for Scheme G2 superimposed over our experimental data.

Based on the fitted rate constants for Scheme G2, several predictions can be made about the kinetic behavior of the nAChR channel in the presence of tacrine. For the open time distribution, predictions of Scheme G2 are relatively straightforward. In any kinetic scheme, the lifetime of a particular state depends on the sum of the rate constants governing exit from that state. Thus, Scheme G2 predicts that the reciprocal mean open time of the channel (τ_{open}) varies linearly with tacrine concentration as follows:

$$\frac{1}{\tau_{open}} = \alpha + T.k_{T+1}, \qquad (7)$$

where α is the channel closing rate, T is the concentration of tacrine and k_{T+1} is the association rate for tacrine. Eq. 7 has the same form as Eq. 5 and comparing the k_{T+1} values in Table VI with the values of k_{T+1} derived from apparent open time plots (Table III) demonstrates excellent agreement between experimental and predicted association rates.

For the closed time distribution, the situation is more complicated because of intercommunication between the open-blocked states with one and two bound tacrines, and between the closed-blocked state and the closed states of the receptor. Considering first the open-blocked states, it is clear that any given channel-block event might consist solely of a dwell in the monoliganded A_2B_T state followed by dissociation of tacrine and return to the open state. Alternatively, it might consist of a dwell in A_2B_T followed by multiple transitions to A_2B_{TT} before return to the open state. These two types of block events are predicted to give rise to two exponential components in the closed-time distribution, but the rate constants describing these exponentials do not relate directly to the lifetime of any individual states in Scheme G2. As described by Colquhoun and Hawkes (1981, 1995), the rate constants (λ_1, λ_2) of these exponentials must calculated by solving the quadratic equation $\lambda^2 + b\lambda + c = 0$, where:

$$-b = \lambda_1 + \lambda_2 = k_{T-1} + k_{T+2}.k_{T-2}$$
$$c = \lambda_1 + \lambda_2 = k_{T-1}.k_{T-2}.$$

Similarly, the relative areas (a_1, a_2) of the two components are given by the formulae:

$$a_1 = \frac{k_{T-1}.(k_{T-2} - \lambda_1)}{\lambda_1.(\lambda_2 - \lambda_1)} \qquad \text{and} \quad a_2 = 1 - a_1.$$

The derivations of these equations are given in full in APPENDIX B. As shown in Fig. 8, Scheme G2 predicts that the component of the closed-time distribution described by λ_1 becomes briefer and that its relative area (a_1) decreases as the concentration of tacrine is increased. However, we could not identify this closed-time component in our experimental data, probably due to temporal overlap of the λ_1 component with closings arising from agonist binding and channel gating (β'). Conversely, Scheme G2 predicts that the component of the closed-time component described by λ_2, increases in duration and relative area (a_2) with increasing tacrine concentration. The time constants of these closings are in excellent agreement with our experimental data (Fig. 8).

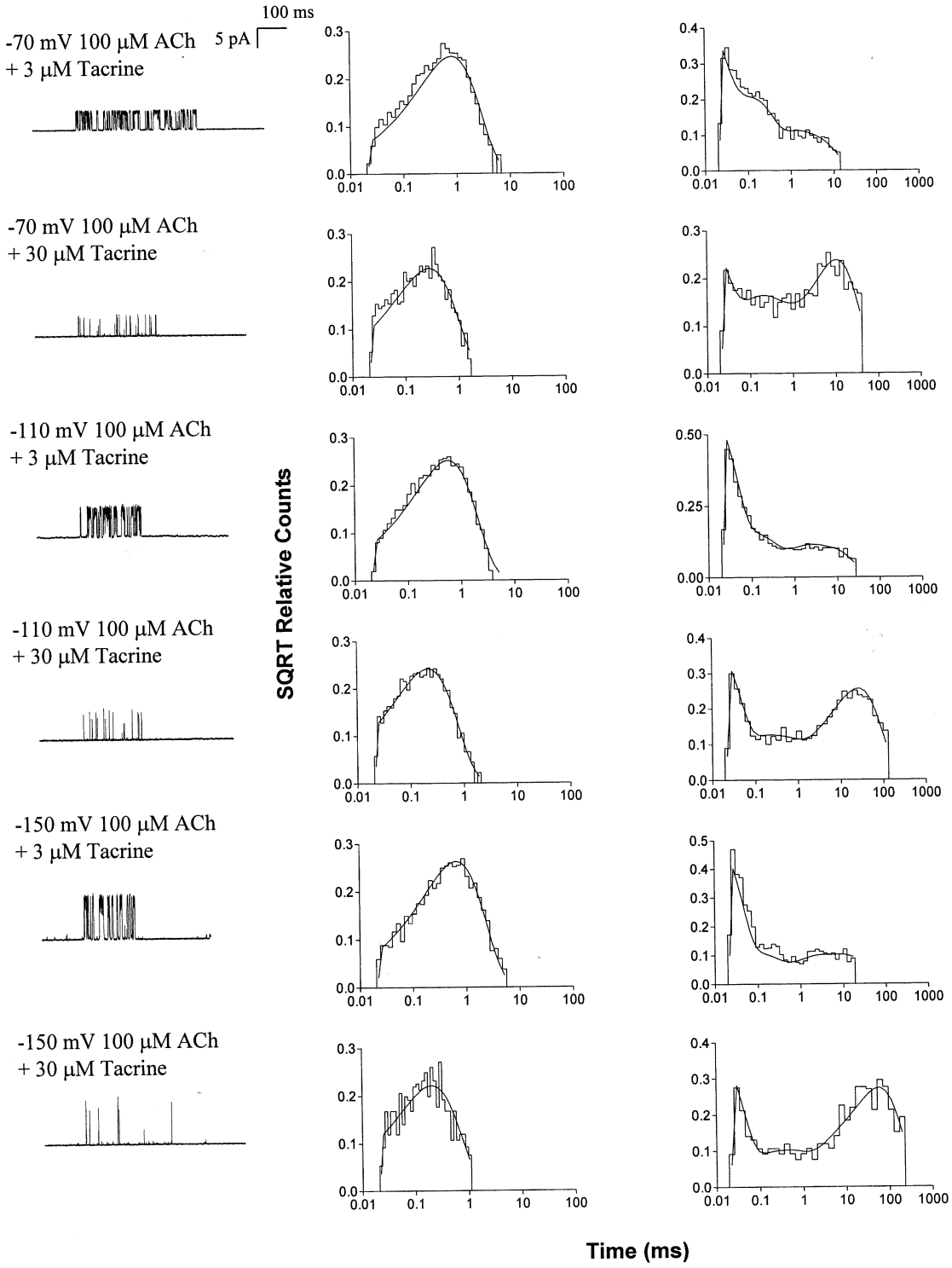

FIGURE 7. Kinetics of activation of nAChRs by 100 μM acetylcholine in the presence of the indicated concentrations of tacrine. Left panels show traces of individual clusters from patches displayed at a bandwidth of 5 kHz. The smooth curves through the open and closed time histograms are theoretical probability density functions calculated from the fitted rate constants for Scheme G2, with parameter values given in Table VI. At each concentration of tacrine, the number of clusters analyzed ranged as follows: −70 mV 44–127, −110 mV 59–136, −150 mV 51–88, whereas the number of events ranged from 4,932–11,580 (−70 mV), 6,020–12,940 (−110 mV) and 3,140–11,904 (−150 mV).

TABLE VI

Kinetic Parameters for the Block of nAChR Channels by Tacrine

	−70 mV	−110 mV	−150 mV
Scheme F4			
k_{T+1}	89 ± 2	107 ± 3	120 ± 3
k_{T-1}	686 ± 25	441 ± 19	297 ± 14
K_{T1}	7.7	4.1	2.5
k_{T+2}	75 ± 7	77 ± 6	82 ± 14
k_{T-2}	535 ± 38	301 ± 15	208 ± 15
K_{T2}	7.1	3.9	2.5
k_{T+3}	7 ± 2	10 ± 2	19 ± 3
k_{T-3}	535 ± 143	210 ± 35	155 ± 24
K_{T3}	76.4	21	8.2
Scheme G2			
k_{T+1}	91 ± 1	114 ± 2	129 ± 2
k_{T-1}	675 ± 21	426 ± 17	290 ± 13
K_{T1}	7.4	3.7	2.2
k_{T+2}	81 ± 7	71 ± 5	78 ± 7
k_{T-2}	596 ± 3	307 ± 14	213 ± 16
K_{T2}	7.4	4.3	2.7
k_{T+3}	154 ± 26	110 ± 45	474 ± 90
k_{T-3}	1,773 ± 384	267 ± 92	231 ± 55
K_{T3}	11.5	2.4	0.5

Parameters were derived from maximum likelihood fitting of Schemes F4 and G2 to single channel data obtained at 100 μM ACh in the presence of 1–60 μM tacrine. Association rate constants are given in units of $\mu M^{-1}\ s^{-1}$ and dissociation rate constants in units of s^{-1} and are expressed ± SE. Parameters governing activation and open channel block of the receptor by ACh were constrained to the values given in Table IV. K_{T1}, K_{T2}, and K_{T3} are dissociation constants calculated from the relevant association and dissociation rate constants, i.e., $K_{T1} = k_{T-1}/k_{T+1}$, and are expressed as μM.

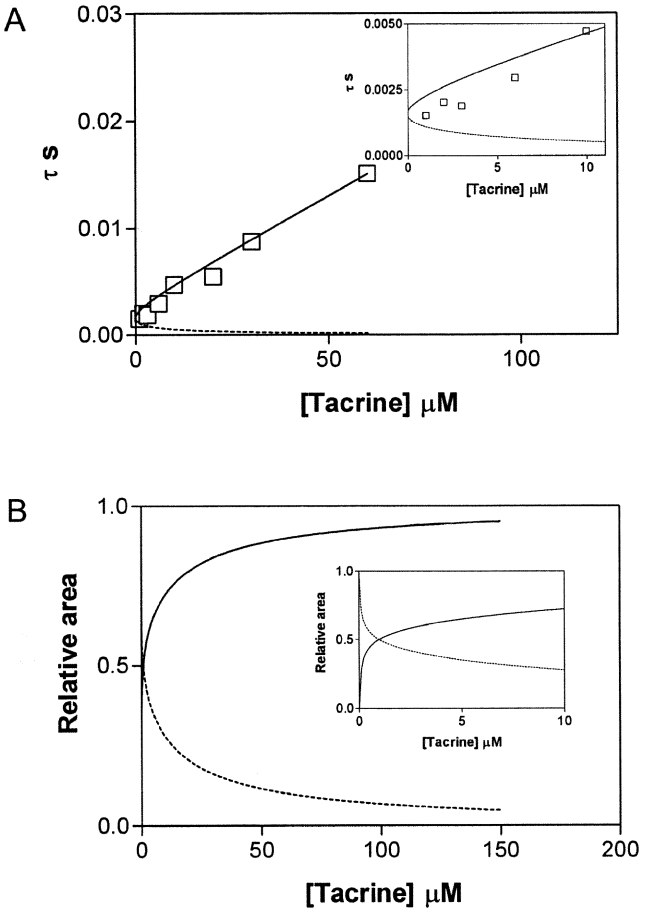

FIGURE 8. Predicted block closed-time distributions for Scheme G2. (A) Data are the observed time constants of closings arising from tacrine block at −70 mV. (Inset) Low concentration range. The lines are the time constants (τ) $1/\lambda_1$ (dashed) and $1/\lambda_2$ (solid) calculated as described in the RESULTS section and in APPENDIX B. (B) Predicted relative areas of the closed-time distribution components arising from λ_1 (dashed) and λ_2 (solid). The lines were calculated as described in the RESULTS section and APPENDIX B. (Inset) Low concentration range.

For the closed-blocked state A_2C_T, the situation is even more complex. In Scheme A, which describes receptor activation in the absence of tacrine, the receptor may shuttle between the C, AC, and A_2C states a number of times before finally opening. In the closed-time histogram this is reflected in an exponential component whose time constant, β′ (the effective channel opening rate), depends on the values of k_{+1}, k_{-1}, k_{+2}, k_{-2}, β, and the concentration of ACh. In Scheme G2, A_2C_T is directly linked to A_2C and thus indirectly to AC and C, predicting that closed channel block should affect the β′ component in a manner that depends on tacrine concentration. This concentration dependence arises because increasing concentrations of tacrine progressively trap the receptor in transitions between the A_2C_T and A_2C states. The probability that a receptor in the A_2C state binds tacrine, as opposed to opening or losing a molecule of ACh, can be calculated thus:

$$P = \frac{k_{T+3}.T}{\beta + k_{-2} + T.k_{T+3}}.$$

At 60 μM tacrine (−70 mV) P = 0.11, suggesting that even at the maximum concentrations of tacrine examined in this study, only marginal changes in β′ should be observed. In agreement with this prediction we found no tacrine-dependent changes in the value of β′ in our experimental data.

A somewhat unexpected finding in our initial analysis was that the tacrine association rates predicted by the blocking frequency were consistently slower than those derived from apparent open time plots. In contrast, previous studies have demonstrated that these methods yield essentially identical results (Ogden and Colquhoun, 1985). To understand these findings in the context of Scheme G2, it is important to realize that while blocking frequency and apparent open time plots are both used to derive the same parameter (k_{T+1}), they make use of very different information. In the apparent open time plot we measure interruption of channel openings by blocking events. Providing these block closings are long enough to be resolved, they will shorten the mean channel open time whether they fol-

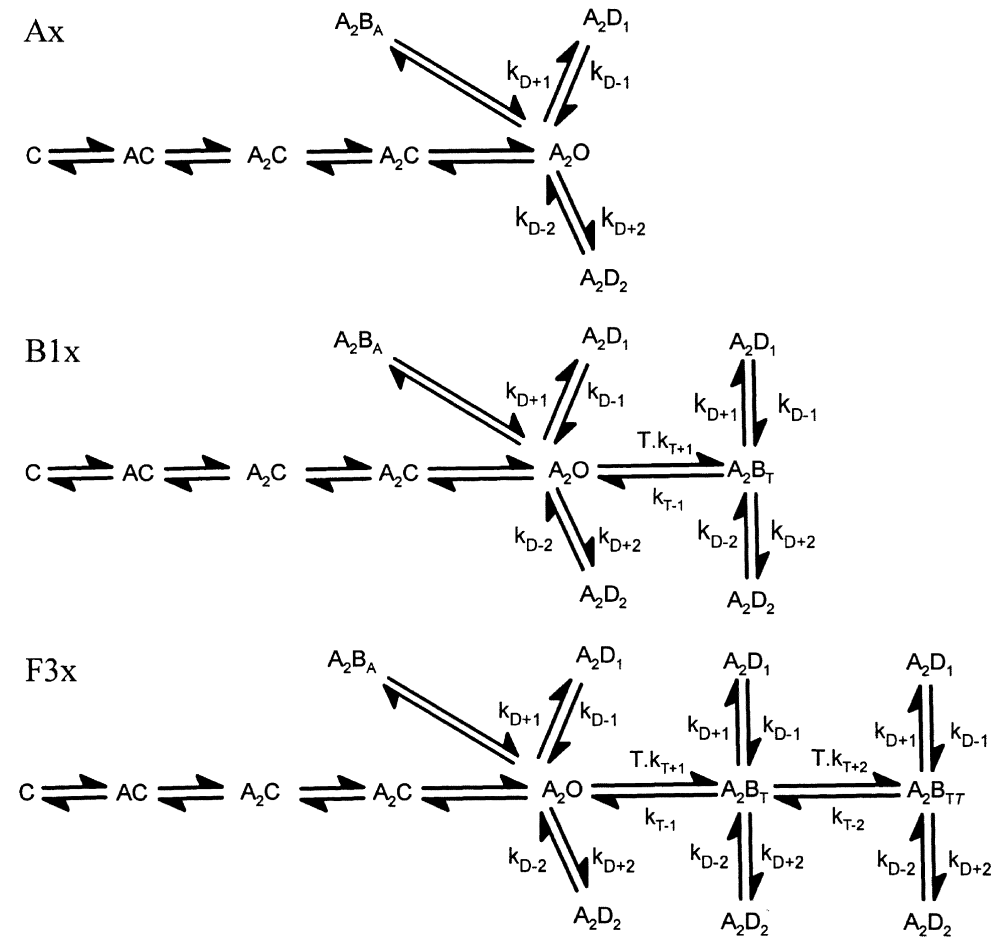

FIGURE 9. Schemes used in simulation experiments. In Schemes Ax, B1x and F3x, k_{D+1}, k_{D-1}, k_{D+2}, k_{D-2} (rate constants governing desensitization and recovery from desensitization), k_{T+1}, k_{T-1}, k_{T+2}, and k_{T-2} were set to the values in Table VII. For clarity, the rate constants governing activation and block of the channel by ACh have been omitted. In the simulations, these were set to the values given in Table IV (−70 mV data).

low a single- or multiple-component distribution. Apparent open time plots are therefore a robust method for deriving values of k_{T+1}. By contrast, the blocking frequency plot requires us to determine the number of block-closings. This can be a problem for mechanisms that yield multicomponent and/or concentration-dependent distributions of block closings. As detailed above, the distribution of block closings predicted by Scheme G2 is described by two exponential functions. One component increases in mean duration and relative area with increasing tacrine concentration, and because this is the only clearly identifiable new component in the closed-time histogram, only closings from this exponential contribute to the block frequency plot. The second exponential component becomes briefer and has a smaller area as the concentration of tacrine increases. This component cannot be identified in the closed-time histogram because it becomes submerged beneath the exponential components that arise from channel gating and agonist binding. Neglect of the brief block exponential, which at 60 μM ACh (−70 mV) still comprises ~10% of all block closings, therefore leads to an underestimation of blocking frequency and hence k_{T+1}.

Effects of Tacrine on Cluster Duration

To allow data to be analyzed using the MIL program, clusters of channel openings corresponding to the activation of single channels must be identified. Our procedure involves selecting groups of openings bounded by long closed times that correspond to periods when all channels in the patch are desensitized. In the absence of tacrine, responses to 100 μM ACh at −70 mV (Fig. 5) revealed three distinct components of closings attributable to desensitization: fast τ_{d1} 2.2 ± 0.8 ms, 1.1 ± 0.3% total closings; medium τ_{d2} 30 ± 7 ms, 0.7 ± 0.2% total closings; and slow τ_{d3} 7,400 ± 3,100 ms, 0.4 ± 0.1% total closings; mean ± SEM of three recordings). In each recording, cluster boundaries are defined using the fastest resolvable type of desensitization closing. At 100 μM ACh, fast desensitization closings are readily identifiable and including them when computing cluster duration yields a mean duration of 37 ± 7 ms (mean ± SEM, $n = 3$). However, the fast and me-

dium rate desensitization closings occur primarily between activation episodes of the same channel so single channel clusters can, in principle, also be defined using the medium or slow desensitization closings. At 100 μM ACh this results in mean cluster durations of 71 ± 17 ms (medium) and 365 ± 33 ms (slow). In the presence of 10 μM tacrine and 100 μM ACh, fast desensitization closings cannot be used to define cluster boundaries because they are obscured by closings due to channel block. The medium and slow desensitization closings, however, can be readily resolved and yield clusters with mean durations of 86 ± 37 ms (medium) and 355 ± 97 ms (slow) (mean ± SEM, $n = 4$). These values are not significantly different from the corresponding cluster durations in the absence of tacrine ($P > 0.7$ by Student's t test). The failure of tacrine to alter cluster duration is consistent with a mechanism in which the receptor can desensitize from open-blocked states at the same rate as from the open-state.

Simulation of Single Channel Data

The concentrations of tacrine used in this study give rise to closed times which overlap with closed times arising from fast and medium onset desensitization. Although desensitization closings make only minor contributions to the closed time histogram, our modelling results might be biased by their inclusion. In particular, we were concerned that (a) improvements in fit relative to the classic sequential model for channel block (Scheme B1), and that (b) the improved fits yielded by Schemes F4–I1 relative to Scheme F3 were due to contamination with desensitization closings. To address this question we simulated single channel open and closed dwell times using the method of Clay and DeFelice (1983). First we expanded Scheme A by adding two desensitized states arising from the diliganded open state (Fig. 9, Scheme Ax) and simulated single channel responses to 100 μM ACh according to the best-fit parameters for Scheme A. We then varied the rate constants governing desensitization to replicate the time constants and weights of the fast and medium rate desensitization closings in our experimental data (final values given in Table VII). Next, we incorporated the fast and medium desensitization closings in Schemes B1 and F3 assuming (a) that desensitization occurs from open or open-blocked states but not closed-states of the receptor and (b) that the binding of tacrine to the receptor did not alter the desensitization rate constants (the expanded schemes, given in Fig. 9 are denoted by the suffix x i.e., Scheme B1x, F3x).

We simulated 5,000 channel openings and closings at 1, 2, 3, 6, 10, 20, 30, and 60 μM tacrine according to Schemes B1x and F3x using the rate constants that gave the best fit of each scheme to our experimental data at −70 mV (Table VII). Next, we selected clusters of openings for analysis as described above and fitted, in turn, Schemes B1, C3, C4, E1, F2, F3, F4, G1, G2, and I1 to each data-set. The log-likelihood values for these fits are summarized in Table VIII.

TABLE VII

Simulation Parameters for Schemes B1x and F3x

	Scheme B1x	Scheme F3x
k_{D+1}	30	30
k_{D-1}	400	400
k_{D+2}	18	18
k_{D-2}	33	33
k_{T+1}	84	96
k_{T-1}	144	655
k_{T+2}	—	61
k_{T-2}	—	497

Data were simulated according to Schemes B1x and F3x using the method of Clay and DeFelice (1983). k_{D+1} and k_{D+2} are rate constants governing the entry of the receptor into the fast and medium duration desensitized states and k_{D-1} and k_{D-2} are the rate constants for exit from those states. k_{T+1} and k_{T+2} are the association rate constants and k_{T-1} and k_{T-2} are the dissociation rate constants for tacrine binding at two sites within the open channel. Values of rate constants governing desensitization were derived by iterative simulation of data according to Scheme Ax, varying the rate constants until the closed time histogram replicated our experimental data obtained at 100 mM ACh (−70 mV values). Values of k_{T+1}, k_{T+2}, k_{T-1}, and k_{T-2} are from the maximum likelihood fits of Schemes B1 and F3 to our experimental data (−70 mV).

Data simulated according to Scheme B1x were well described by Scheme B1 with fitted parameters within 9% of the input values. Schemes C3, E1, and F2 did not produce convergent fits to Scheme B1x data but improved fits relative to Scheme B1 were obtained with Schemes F3, F4, G1, G2, and I1. This improvement pre-

TABLE VIII

Log-likelihood Values Derived from Scheme Fitting to Simulated Data

	Data generated using	
	Scheme B1x	Scheme F3x
Scheme B1	235,984	232,928
Scheme C3	Did not converge	233,480
Scheme C4	235,984	233,069
Scheme E1	Did not converge	234,350
Scheme F2	Did not converge	234,334
Scheme F3	235,989	234,426
Scheme F4	235,989	234,436
Scheme G1	235,989	234,462
Scheme G2	235,989	234,426
Scheme I1	235,989	234,436

Log-likelihood values were generated by fitting schemes to data simulated using Schemes B1x and F3x. Schemes B1x and F3x incorporate two desensitized states leading from the open and open-blocked states. For each scheme, channel openings and closings were simulated for 100 μM ACh in the presence of 1–60 μM tacrine using the method of Clay and DeFelice (1983). Clusters were defined and selected for analysis as described in the text.

sumably arises because the fitting process interprets the desensitization closings in terms of the additional closed states afforded by more complex models. However, the increase in log likelihood for Schemes F3, F4, G1, G2, and I1 versus Scheme B1 was much smaller with the simulated data (five LL units) than with our experimental data (~2,000 LL units) and the fitted values for k_{T+2}, k_{T+3} and k_{T+4} were in all cases very small ($<2.5\ \mu M^{-1}\ s^{-1}$) with errors >50%. Further, the fitted values for k_{T+1} and k_{T-1} were in all cases within 15% of the corresponding input values from Scheme B1. Thus, with our experimental data, the substantial improvements in fit obtained with two-site relative to one-site models are not artifacts caused by receptor desensitization.

Similarly, fits of Scheme F3 to data generated using Scheme F3x yielded excellent agreement between the fitted parameters and the rate constants used to parameterize the scheme (maximum deviation of 4%). Relative to Scheme F3, improved fits were obtained with Schemes F4, G1, and I1 but not with Scheme G2 or any other model tested. These improvements presumably arise because the fitting process accounts for some of the desensitization closings using the additional blocked state in Schemes F4, G1, and I1. Unlike our results with Scheme B1x, however, the increases in log likelihood value with Schemes F4, G1, and I1 are of similar magnitude to improvements in fit, relative to Scheme F3, that are obtained when these schemes are fitted to our experimental data. Thus, our simulation results suggest that the likelihood values of models in which tacrine is postulated to bind randomly to two sites in the open channel or which allow for channel closing with tacrine bound, may be significantly inflated by the inclusion of desensitization closings in our data.

Scheme G2, on the other hand, does not improve fits (relative to Scheme F3) to data simulated using Scheme F3x. This indicates that for our simulated data, desensitization closings cannot be accommodated by the addition of closed-blocked states. By contrast, Scheme G2 does produce an improved fit relative to Scheme F3 with our real patch clamp data. Based on our results with simulated data, this improvement is unlikely to arise from the presence of desensitization closings and must therefore be due to dwells of the receptor in the closed-blocked state.

Voltage Dependence of Tacrine Binding

Fits of Scheme G2 to our data revealed that the dissociation constants (calculated from the fitted rate constants) for the two tacrine binding sites in the open channel decreased as the membrane potential became more hyperpolarized (Table VI). Applying the Woodhull equation (Woodhull, 1973) to these data yields electrical distances of 0.38 for the first binding site and 0.32 for the second site. Binding to the closed channel also shows apparent voltage sensitivity but inspection of the association and dissociation rate constants at this site reveals that they do not vary in a consistent manner.

DISCUSSION

Open channel block of the nAChR has classically been described by a simple sequential mechanism in which blockers bind to a single site within the open channel of the receptor (Scheme B1). For many compounds, e.g., QX-222 (Charnet et al., 1990), epibatidine (Prince and Sine, 1998a), and pyrantel (Rayes et al., 2001), such models provide a good, quantitative description of the interactions between the blocker and the nAChR channel, at least at lower concentrations of blocker. In other studies, simple sequential models have failed to explain fully the kinetics of nAChR block (Neher, 1983; Papke and Oswald, 1989; Dilger et al., 1997; Evans and Martin, 1996), but in most cases the merits of alternative models have not been explored systematically.

In our current study we found that the simple sequential model for open channel block can describe accurately the concentration-dependent decrease in channel open time produced by tacrine, but fails to account for the concentration dependence of the closed-time distribution. The simple sequential mechanism for open channel block predicts that the duration of closings due to channel block should depend solely on the dissociation rate constant of the blocker and thus should not vary with blocker concentration.

Concentration dependence of channel closings requires that tacrine stabilizes a state of the receptor in which ion flux does not occur. Thus, there are two general classes of mechanism that could explain the effect of tacrine on the open and closed time distributions. The first class requires that tacrine binds to and blocks the open channel of the nAChR, but also binds to a closed state of the receptor. The second class involves multiple binding sites for tacrine on the open state of the receptor. Below, we evaluate a variety of kinetic models within these two general frameworks.

Models Involving Interactions with Closed States

Parallel block mechanisms. The first general mechanism we examined (Mechanism C) allows tacrine to bind to the channel in both the open (A_2O) and closed state (A_2C) and allows channel gating to occur with tacrine bound (Adams, 1977). This type of mechanism has been termed "parallel block" because it provides two parallel pathways for the receptor to switch between open and closed states. In studies of fetal mouse receptors in a clonal cell line, Papke and Oswald (1989) found that parallel block provided a quantitatively better description than classic sequential block to explain the kinetics of tetracaine, phencyclidine, and *N*-allyl-

normetazocine on single channel currents activated by low concentrations of ACh. A similar mechanism was also proposed by Neely and Lingle (1986) to explain the kinetics of chlorisondamine block.

Our first derivative of the parallel block mechanism was Scheme C1 in which we assumed (a) that the channel could open and close at the same rate irrespective of whether tacrine was bound and (b) that the rate constants governing tacrine binding were the same in the open and closed states of the receptor. This mechanism yielded an even worse description of our data than the sequential model (Scheme B1). Next, we tested a mechanism (Scheme C2) in which the constraints on channel gating and tacrine binding were removed. However, we found that fits of Scheme C2 to our data did not yield a full, parallel block mechanism. Instead, Scheme C2 converged with values of k_{T+2} and k_{T-2} (association and dissociation rates governing tacrine binding to the closed channel) close to zero and yielded the same log-likelihood value as Scheme C3 (in which it was assumed that tacrine could not bind to the closed channel). The mechanism described by Schemes C2 and C3 has two main characteristics. First, tacrine associates only with the open state of the channel. Second, when the channel has bound tacrine it can access an additional nonconducting state from which tacrine cannot dissociate. Although Schemes C2 and C3 both yield better fits than the classic sequential model (Scheme B1, see Table V and Fig. 3) neither predicts concentration dependent block closings. It is therefore not intuitively obvious from where the improvement in fit obtained with these schemes arises (they probably work better by merely including a second closed state). Possible identities of the additional nonconducting state are discussed below in the context of two site models.

We also examined a variation of the parallel block mechanism that assumes that the channel cannot gate with tacrine bound (Scheme C4), but which allows tacrine to bind to the closed state of the receptor. In parallel block mechanisms the effective channel opening rate, β', will vary with tacrine concentration because the A_2C_T state is connected directly to A_2C and thus indirectly to AC and C. Effects on β' will be most pronounced when k_{T-2} is much faster than β^* (channel opening rate with tacrine bound) e.g., when β^* and α^* are set to zero: as the concentration of tacrine is raised the receptor will spend progressively more time shuttling between the A_2C_T and A_2C states. Although Scheme C4 also yielded an improved fit relative to Scheme B1, two factors suggest that this type of mechanism is unlikely. First, examination of closed time histograms (Fig. 5 A) shows that the component of the closed-time distribution attributable to β' (mean duration 100–200 μs) is unaffected by tacrine. Second, for β' to be lengthened significantly by tacrine, [tacrine].k_{T+2} must approach or exceed ($\beta + k_{-2}$), which for ACh at −70 mV is ∼73,000 s^{-1}. Tacrine-induced closings are readily distinguishable in the closed time histogram and increase approximately linearly in duration with increasing concentration. To explain these findings at, for example, 2 μM tacrine, requires k_{T+2} to be >36,000 $\mu M^{-1} s^{-1}$. This is ∼36-fold faster than the upper limit for a diffusion-limited association reaction and thus is physically unreasonable.

Competitive Interactions

The second type of model we considered combines sequential open channel block with a competitive interaction at the ACh binding sites (Scheme D1). This model was of interest because ligand binding studies on human cortical nAChRs (Perry et al., 1988) and whole brain tissue (Hunter et al., 1989) provided evidence for competitive binding at neuronal nAChR ACh recognition sites, with K_d values in the low micromolar range. However, more recent studies suggest a complex mode of interaction with neuronal receptors. Svensson and Nordberg (1996) and Svensson (2000) found that chronic treatment with tacrine modulates receptor number in clonal SHSY5Y and M10 cells and speculated that this may involve interaction at an allosteric site in addition to the agonist binding site. A study on α4β2 and α4β4 subunit combinations (Zwart et al., 2000), however, suggested that tacrine binds to the agonist recognition site and acts as a coagonist with ACh, in addition to blocking the receptor in the open state. Although it is not always possible to extrapolate results obtained with neuronal AChRs to the muscle receptor, competitive interactions combined with open channel block could, in theory, explain our present results. Thus, we tested the hypothesis that tacrine competes with ACh. We found three lines of evidence which together strongly suggest that tacrine does not exert its effects via a competitive mechanism. First, we fitted a model combining competitive interactions with open channel block (Scheme D1). Although this mechanism yielded a significantly better fit at all membrane potentials than the classic sequential model for open channel block, it ranked poorly compared with other mechanisms. The poor fit likely results because competitive interactions, like parallel block mechanisms, are predicted to alter the value of β'. Second, we observed that the decrease in P_{open} produced by 10 μM tacrine at 100 and 300 μM ACh was essentially the same. A competitive mechanism predicts less inhibition at higher concentrations of agonist. Finally, we performed ligand binding assays to determine directly the Ki for tacrine competition against the initial rate of [^{125}I]-labeled α-bungarotoxin. The affinity of tacrine in this assay is 300 μM, much higher than the IC_{50} value determined in patch-clamp experiments.

Multiple Block Sites

We next examined general classes of mechanism involving multiple binding sites for tacrine within the open receptor channel. The first model we examined (Scheme E1) postulates that there are two block sites at different depths within the channel. Tacrine binds first to the upper site, thereby blocking the channel, and then can either dissociate or diffuse down the channel to the deeper site. A second molecule of tacrine can then bind to the upper site, trapping the first molecule in the channel. Similar models have been used to fit data for block of nAChRs by ACh itself (Maconochie and Steinbach, 1995) as well as the anthelmintic agent, morantel (Evans and Martin, 1996). As in both of these previous studies, Scheme E1 gave superior fits to our data compared with the classic sequential scheme for open channel block ($P < 0.0001$ by LRT).

We also considered a general mechanism in which tacrine can associate randomly with two binding sites in the open state of the receptor (Mechanism F). To our knowledge, models involving random association at two binding sites have not been used to describe open channel block previously, but a derivative of this mechanism, in which the two sites were assumed to have very different affinities, was examined by Maconochie and Steinbach (1995) as a possible mechanism for block by ACh. The first model we tested was Scheme F1, which allows random association at the two sites and permits allosteric interactions. We found that Scheme F1 yielded excellent fits to our data with log-likelihoods 1,600–2,600 U higher than the sequential model for open channel block ($P < 0.0001$ by LRT). However, the fitted values for k_{T+3}, k_{T+4}, k_{T-3}, and k_{T-4} were ill-defined and very slow. This prompted us to examined three simplified versions of Scheme F1. In Scheme F2 we assumed full independence of the tacrine binding sites. This model produced significantly worse fits to our data ($P < 0.0001$ by LRT) than Scheme F1. Next, we assessed a model in which the state A_2B_T was eliminated (Scheme F3). Again, we found that this model did not perform as well as Scheme F1. Finally, in Scheme F4, only the transitions governed by k_{T+4} and k_{-4} were eliminated. We found that this model gave equal log-likelihood values to those obtained with Scheme F1 and that the fitted parameters had much lower error estimates. The rate constants derived from fits to Scheme F4 (Table VI) describe a model in which the two unoccupied tacrine binding sites differ greatly in affinity. The binding of tacrine to the higher affinity site enhances the affinity of the remaining site, but when the low affinity site is occupied first, occupancy of the high affinity site is prevented. Thus, the two sites interact with positive cooperativity but the allosteric interaction depends on the order in which the sites become occupied. One possible physical correlate of this model would involve two binding sites at different depths within the channel. Tacrine can interact with either site, but association with the upper site is allosterically enhanced by occupancy of the lower site. On the other hand, if the upper site is the first to bind tacrine, access to the lower site is prevented by steric hindrance. However, while consideration of log-likelihood values clearly demonstrates that Scheme F4 provides a good description of our data, our results from simulation experiments do not provide support for this model and suggest that the apparent superiority of Scheme F4 over Scheme F3 may be due to inclusion of channel closings arising from fast and medium modes of receptor desensitization.

More Complex Models

Thus far we have discussed three distinct types of kinetic model which yielded improved fits to our data relative to the sequential model: a scheme in which the channel can gate with tacrine bound, a scheme involving interactions with the diliganded closed state of the receptor and a series of models involving two binding sites on the open state of the channel. Therefore, we wished to see if combining features of these types of model into a single mechanism would yield further improvements in the description of our data. The first series of models we considered (Mechanism G, Fig. 3) extends the parallel block mechanism (Mechanism C) by adding a second binding site for tacrine in the open state of the receptor. Dilger et al. (1997) found that this type of model provided a good description of the block kinetics of pentobarbitone at the mouse fetal-type nAChR. Like tacrine, pentobarbitone produces concentration-dependent closed times. Based on our results from single-site parallel block models, we considered three schemes within this general framework. The first model we examined, Scheme G1, gave substantial improvements in fit compared with both its parent schemes (Schemes F3 and C3). This model features two binding sites for tacrine in the open channel and an additional "dead-end" state that the receptor can access when the channel has bound a single molecule of tacrine, but from which tacrine cannot dissociate. At least three physical correlates of Scheme G1 can be envisioned. First, the dead-end state may arise because the channel closes, and traps tacrine in its binding site. Second, in our modelling experiments we have assumed that the block of the channel by tacrine and ACh are mutually exclusive. However, the dead-end state in Scheme G1 might also arise because ACh binds to a site within the channel thereby preventing tacrine from escaping. Finally, the additional state in Scheme G1 might correlate with a desensitized state. We consider this the most likely explanation because in our simulation experiments, Scheme G1 gave much better fits than Scheme F3 to data generated using Scheme F3x (i.e., Scheme F3 incorporating desensitization closings). Thus, the apparently superior

fits obtained when Scheme G1 was applied to our patch-clamp data may derive from the inclusion of desensitization closings in our data.

Next, we fitted Scheme G2 to our data. This model assumes that tacrine can bind to both the open and closed states of the channel but does not permit channels occupied by tacrine to open or close. We found that Scheme G2 gave a superior fit compared with Scheme G1 at −70 and −150 mV but not at −110 mV. Finally, we examined Scheme G3, which describes a full parallel block mechanism that allows binding of tacrine to the open and closed states and permits channel gating with tacrine bound. At −70 mV and −150 mV fits of Scheme G3 yielded values of β* and α* close to zero and therefore simplified to Scheme G2. Conversely, when Scheme G3 was fitted to our −110 mV data it yielded parameter values of k_{T+3} and k_{T-3} close to zero and simplified to Scheme G1. Thus, consistent with our results from single site models, our data do not appear to be compatible with parallel block mechanisms.

Within the framework of Mechanism G, Scheme G2 produced the best fit to two out of our three datasets. Therefore, we used Scheme G2 as the starting point for our final two models. First we expanded Scheme G2 to allow binding of tacrine to two sites on the closed receptor (Scheme H1). Addition of the extra closed-state binding site did not, however, produce any significant improvements in the fits. Finally, we examined Scheme I1, which combines Schemes G2 and F3, allowing tacrine to bind randomly to two sites in the open channel and to interact with a single site on the closed state of the receptor. Overall, Scheme I1 gave the highest log-likelihood values of any model tested in this study. However, as with Schemes F3 and G1, the results of our simulations suggest that the improvements generated by the incorporation of the A_2B_T state are most likely due to the inclusion of desensitization closings in our data.

Our simulated data reveal that fits to models which postulate the binding of tacrine to closed as well as open states (Scheme G2) do not appear to be greatly influenced by desensitization closings, unlike models in which tacrine can bind randomly to two sites within the channel (Schemes F1, F4, I1) or which contain "dead-end" states (Scheme G1). Assuming that this finding can be extrapolated to our experimental data, the model that provides the best, unbiased description of our data is therefore Scheme G2. A simple interpretation of Scheme G2 is a mechanism in which there are two allosterically coupled binding sites for tacrine within the channel. One of these binding sites is accessible to tacrine in the closed as well as the open state of the channel, but the second site can be occupied only when the channel is open and tacrine has bound to the first site.

Nature and Location of the Tacrine Binding Sites

Conformation of the "blocked" state. Thus far we have assumed that the "blocked" states in our models arise from the physical plugging of the channel by tacrine. However, many noncompetitive inhibitors of the nAChR have also been reported to cause receptor desensitization as well as channel block (Benoit and Changeux, 1993; Arias, 1996) and distinguishing between these modes of inhibition is problematic (Clapham and Neher, 1984). It is therefore possible that tacrine may have a similar dual action i.e., that one or both of the "blocked" states in Scheme G2 are in fact new desensitized states induced by tacrine. From our modelling data, we cannot distinguish between channel block and desensitization because our models identify states by only connectivity and conductance i.e., a "blocked" state is identified as a nonconducting state that the channel enters when tacrine binds and this description applies equally well to a desensitized state. However, three lines of evidence presented in this paper point toward a site of action within the channel lumen and argue against tacrine affecting receptor desensitization. First, our binding studies demonstrate that tacrine does not cause receptor desensitization: at the concentrations used in this study it acts solely as a low potency competitive antagonist (Ki 300 μM). Second, the actions of tacrine are voltage dependent, suggesting a site of action within the membrane field. Similar to our observations with tacrine, a study with chlorpromazine by Benoit and Changeux (1993) found that its desensitizing actions were insensitive to membrane potential, whereas its channel blocking actions were voltage sensitive. Finally, tacrine does not affect cluster duration. Cluster duration is inversely proportional to the desensitization rate of the receptor (Sakmann et al., 1980; Auerbach and Akk, 1998). However, these findings leave open the possibility that tacrine stabilizes or induces a short-lived desensitized state that does not alter agonist affinity in ligand binding studies. A similar mechanism was proposed recently to explain the actions of the quinacrine at the mouse adult nAChR (Spitzmaul et al., 2001).

Location of the tacrine binding sites. Apparent electrical distances derived from the Woodhull equation (Woodhull, 1973) have been used extensively to infer the locations of blocker binding sites within ion channels. Assuming that the field drops linearly across the membrane, our data suggest (a) that both tacrine binding sites are located at similar depths in the open channel and (b) that the sites with which tacrine's amino group interacts are located about one third of the way down the channel. This is similar to the electrical distance calculated for quinacrine (Adams and Feltz, 1980). By contrast, the classic open channel blocker QX-222 binds at an electrical distance of ∼0.8 (Neher

and Steinbach, 1978; Pascual and Karlin, 1998). QX-222 is membrane impermeant due to its quaternary amine structure, suggesting that it must act on the nAChR from the extracellular side of the cell membrane. As the electrical distances calculated for tacrine place its binding sites more extracellular than that of QX-222, it seems reasonable to conclude that tacrine also accesses the nAChR channel from the extracellular side.

At the amino acid level, clues about the structure of the tacrine binding sites can be drawn from previous photoaffinity labeling studies. For example, quinacrine, which is structurally similar to tacrine and binds at a similar electrical distance, labels two residues at the extracellular end of M1: αR209 and αP211 (for review see Arias, 1996). An electrical distance of ~0.3 also places the tacrine binding sites at a depth close to the ring of conserved valine residues at position 13′ in the second transmembrane domain (the terminology of Miller [1989] numbers the NH_2 terminus of M2 as 1′. Therefore, position 13′ corresponds to αV255 and its equivalents in β, δ, and ϵ). By analogy with other open channel blockers such as QX-222 and ACh itself, the voltage sensitivity of tacrine binding suggests that tacrine binds in its protonated form. However, position 13′ residues in the β and δ subunits of the Torpedo receptor are photoaffinity labeled by the hydrophobic probe 3-(Trifluoromethyl)-3(-*m*-[^{125}I]iodophenyl)diazirine. As tacrine is a relatively weak base (pKa 9.4) we cannot completely rule out the possibility that it is the unprotonated form of the drug that binds to the channel, with the apparent voltage sensitivity arising from subtle changes in channel structure at more hyperpolarized potentials. Ultimately, delimiting the binding site for tacrine may require an approach similar to that adopted by Charnet et al. (1990) who localized the binding site for QX-222 by making nonconservative point mutations at key positions within the channel domain and determining their effects on channel kinetics.

Voltage Dependence of ACh Binding and Channel Gating

A prerequisite for our analysis of tacrine block kinetics was that we first gained a detailed picture of the interactions of acetylcholine itself with the receptor. Thus, at each membrane potential we analyzed recordings made over a range of ACh concentrations and determined the rate and equilibrium constants governing activation and block of the receptor by ACh. These experiments, which to the best of our knowledge are the first to examine the voltage dependence of human adult nAChR kinetics, reveal broadly similar behavior to nAChRs characterized previously in terms of channel gating and channel block by ACh, but intriguing differences in the voltage dependence of ACh binding at the agonist binding sites. Below, we discuss our findings in more detail.

First, the affinity of ACh for its channel block site increased with increasing hyperpolarization (*e*-fold/66 mV). This is not surprising, as block of the channel by ACh is presumed to involve a site within the membrane field. We found that changes in affinity for this site mainly involved an increase in the ACh association rate and that the ACh dissociation rate was essentially voltage insensitive. This is in agreement with results from fast-agonist application experiments (Maconochie and Steinbach, 1995), but stands in contrast to the findings of Sine and Steinbach (1984), who observed strong voltage dependence of both association and dissociation rates for suberyldicholine block.

Second, we observed voltage dependence of the equilibrium constant, Θ, governing channel opening. In agreement with previous studies (Colquhoun and Sakmann, 1985; Auerbach et al., 1996) we found that Θ increased with hyperpolarization and that this arose primarily from decreases in the channel closing rate, α (*e*-fold/156 mV), with only modest increases in the channel opening rate, β (*e*-fold/1067 mV). Auerbach et al.(1996) postulated that the voltage dependence of α arises because a charged moiety moves through the membrane field during channel closure and that this charge is carried by the nAChR protein itself rather than by bound ACh.

Finally, and unexpectedly, we found that the dissociation rates for ACh at the two agonist binding sites decreased with membrane hyperpolarization, with modest decreases also in the association rates (k_{+1} *e*-fold/188 mV, k_{-1} *e*-fold/99 mV, k_{+2} *e*-fold/467 mV, k_{-2} *e*-fold/119 mV). Although there has been only limited investigation of the voltage dependence of ACh binding, previous studies on frog, mouse, and *Torpedo* receptors (Colquhoun and Sakmann, 1985; Auerbach et al., 1996, Sine et al., 1990) have found k_{-2} (the rate constant governing dissociation of ACh from its low affinity binding site) to be essentially voltage insensitive, in contrast to our present findings. Although structural data (Miyazawa et al., 1999) place the agonist binding site well outside the membrane field, it has long been recognized that conformational changes involving structural elements within the membrane field (i.e., channel opening and desensitization) are tightly coupled to the agonist binding sites and can produce dramatic changes in agonist affinity. We speculate that in human adult nAChRs, the structural machinery that couples agonist binding to channel gating and desensitization may also couple the agonist binding sites to an element within the membrane field that senses the potential difference across the cell membrane.

Comparison of the Maximum Likelihood Method with Other Methods of Analyzing Block

Previous single channel studies of nAChR channel block for the most part, have examined the effects of

blockers on parameters such as open, burst, and block duration and blocking frequency. These types of analysis can yield results that are difficult to interpret mechanistically and have only limited sensitivity in terms of their abilities to discriminate between kinetic models. For example, models E1–F4, G2, H1, and I1 each predict linear relationships between tacrine concentration and $1/\tau_{app}$, constant open-time per burst, an increase in burst duration, and concentration dependence of the block-closed time.

To the best of our knowledge, the present study is the first heuristic study of nAChR channel block to make use of maximum likelihood scheme fitting to single channel data. In contrast with previous methods, maximum likelihood fitting offers the ability to discriminate between even very closely related kinetic schemes. The main drawbacks of the maximum likelihood method are that (a) it requires detailed knowledge of the parameters governing agonist interactions with the receptor and (b) it requires the use of agonist concentrations that produce clearly defined clusters, i.e., concentrations that produce significant levels of desensitization. However, these limitations can be overcome with appropriate controls and our present results indicate that maximum likelihood fitting is a sensitive and robust technique for analysis of channel block.

In summary, this study demonstrates that the kinetics of tacrine cannot be explained by the classic sequential model for open channel block and are instead consistent with a model in which tacrine binds to two sites within the open channel and to a single site on the closed channel. Our results underline the complexity of channel block at the nAChR and suggest that our picture of open channel block of the receptor may require revision.

APPENDIX A

The classic sequential mechanism for open channel block (Fig. 3, Scheme B1) has simple connectivity and predicts a linear relationship between the reciprocal of the mean channel open duration (τ_{open}) and the concentration of open channel blocker (T):

$$\frac{1}{\tau_{open}} = \alpha + T.k_{T+1}, \qquad \text{(A1)}$$

where α is the channel closing rate and k_{T+1} is the association rate for tacrine.

Plots of Eq. A1 can be used to derive values of α and k_{T+1} but it is first necessary to correct apparent mean open durations for unresolved dwells in the closed states. These missed closings result in the concatenation of successive channel openings and thus in overestimation of τ_{open}. In the present study, however, this correction is not possible because the partially resolved brief closings that arise from channel gating are of a similar duration to those that arise from block of the channel by ACh itself. Below we demonstrate that for our present data, open time correction is unnecessary and that plots of reciprocal apparent mean open time (τ_{app}) against tacrine concentration also yield a straight-line with a slope approximating $k_{T+1.}$

TABLE IX

Parameters Describing Unblocked Closed State p.d.f for Scheme B1

	Membrane Potential		
	−70 mV	−110 mV	−150 mV
λ_f (s^{-1})	79,317	71,697	70,352
λ_m (s^{-1})	27,337	19,774	18,384
λ_s (s^{-1})	8,543	7,978	8,506
a_f	0.61	0.71	0.78
a_m	0.09	0.11	0.08
a_s	0.3	0.18	0.14
Z_f	0.17	0.26	0.34
Z_m	0.07	0.14	0.14
Z_s	0.76	0.6	0.52

The rate constants (λ) and relative areas (a) of the fast, medium, and slow exponential components of the unblocked closed state p.d.f were calculated at a concentration of 100 μM ACh as described by Colquhoun and Hawkes (1981). The relative contribution to the total time encompassed by the p.d.f (Z) was calculated using Eq. A4.

Closed Time Distribution for Scheme B1

Scheme B1 predicts three exponential components in the closed time histogram due to entry of the channel into the "C" states (C, AC and A_2C). We term these components "fast," "medium" and "slow," but it is important to realize that the mean durations of these components vary with agonist concentration.

As the C, AC, and A_2C states are interconnected, the rate constants (λ_f, λ_m, λ_s) and relative areas (a_f, a_m, a_s) of the fast, medium, and slow exponential components do not relate in a straightforward manner to individual rate constants in Scheme B1 (The definitions of the rate constants and concentration symbols used in Scheme B1 are set out in the main body of this paper [Fig. 3]), and must be derived by solving a cubic function. The derivation of this function closely follows the method used by Colquhoun and Hawkes (1981) for the allosteric agonist mechanism (defined as mechanism 3.1 in their paper) and will not be repeated here. In Table IX we set out the values of the rate constants and relative areas at 100 μM ACh (−70 mV) calculated using the parameters for ACh activation in Table IV.

Once the rate constants and relative areas of the fast, medium and slow components are known, one can readily calculate the relative fraction of closings in each component (F_f, F_m, and F_s, respectively) that is resolved given a dead-time of r:

$$F_f = e^{-\lambda_f r}$$

$$F_m = e^{-\lambda_m . r}$$

$$F_s = e^{-\lambda_s r}$$

Thus, the fraction (F_c) of all resolved closed intervals is given by:

$$F_c = a_f.F_f + a_m.F_m + a_s.F_s,$$

and the apparent closing rate of the channel

$$\alpha_a = F_c.\alpha.$$

Similarly, the fraction of closings due to ACh block that is resolved (F_A) is

$$F_A = e^{-r.k_{B-1}},$$

and the apparent blocking rate for ACh (k_{Ba}) is

$$k_{Ba} = F_A.k_{B+1}.$$

Assuming, further, that all closings due to tacrine block are resolved, an expression for the total time spent in A_2O (τ_i) within a resolved opening is therefore:

$$\tau_i = \frac{1}{\alpha_a + A.k_{Ba} + T.k_{T+1}}. \quad \text{(A2)}$$

However, resolved openings also contain a finite contribution (τ_u) from unresolved closings and ACh block closings. Therefore the total mean duration of an apparent opening (τ_{app}) is:

$$\tau_{app} = \frac{1}{\alpha_a + A.k_{Ba} + T.k_{T+1}} + \tau_u$$

and

$$\frac{1}{\tau_{app}} = \frac{\alpha_a + A.k_{Ba} + T.k_{T+1}}{1 + \tau_u(\alpha_a + A.k_{Ba} + T.k_{T+1})}.$$

Thus, when τ_u is small compared with the total time spent in A_2O (τ_i), the reciprocal of the mean apparent open time will be linearly related to the concentration of tacrine:

$$\frac{1}{\tau_{app}} = \frac{1}{\tau_i} = \alpha_a + A.k_{Ba} + T.k_{T+1} = \frac{1}{\tau_0} + T.k_{T+1}, \quad \text{(A3)}$$

where τ_0 is the apparent mean open time in the absence of tacrine. This is a useful general result because it allows the estimation of blocker association rates at high concentrations of agonist i.e., under conditions where rates of opening of the channel and block of the channel by the agonist compromises distort the true channel open time.

Estimation of the Error Magnitude for Scheme G2

Scheme G2 (Fig. 3) also predicts that apparent open time obeys Eq. A3. Thus, the errors involved in applying Eq. A3 to our data can be estimated from our derived rate constants for Scheme G2. The first step in this calculation requires us to determine the equilibrium occupancy of A_2O (E_O), the unresolved fraction of the equilibrium occupancy of A_2B_A (E_{Bu}), and the fraction of the "C" closed states that is unresolved (E_{Cu}). E_O and E_{Bu} are relatively straightforward:

$$E_O = \frac{A_2O}{A_2O + A_2B + C_{total} + T_{total}}$$

$$E_{Bu} = \frac{A_2B_A.\pi}{A_2O + A_2B + C_{total} + T_{total}},$$

where:

$$C_{total} = C + AC + A_2C. = C + \frac{C.A}{K_1} + \frac{C.A^2}{K_1.K_2}$$

$$A_2O = \frac{C.\theta.A^2}{K_1.K_2}$$

$$A_2B_A = \frac{C.A^3\theta}{K_1.K_2.K_{BA}}$$

$$T_{total} = \frac{A_2O.T}{K_{T1}} + \frac{A_2O.T^2}{K_{T2}K_{T1}} + \frac{A_2C.T}{K_{T3}}$$

$$\pi = k_{B-1}.\int_0^r t.e^{-t.k_{B-1}}dt$$

and θ is the equilibrium constant for channel gating, K_1, K_2, and K_{BA} are equilibrium dissociation constants for ACh at the low and high affinity agonist binding sites and the channel block site respectively, C_{Total} and T_{Total} are occupancy functions for the closed- and blocked-states respectively, and π is the proportion of time missed.

The use of π rather than the more familiar fractional number of closings is important because a given number of closings with durations less than the dead-time will distort the apparent open time less than the same number of closings with durations greater than the dead-time.

Calculation of E_{Cu} requires a little more work because the rate constants and areas of the relevant exponential components in the closed time histogram do not relate to individual states of the receptor. Our first task is to calculate the equilibrium occupancy of the "C" closed states (E_C).

$$E_C = \frac{C_{total}}{A_2O + A_2B + C_{total} + T_{total}}.$$

For each of the three "C" closed state exponentials,[1] we must then calculate the proportion (π_λ) of the total unresolved time encompassed by that exponential.

$$\pi_f = \lambda_f . \int_0^r t . e^{-t.\lambda_f} dt \qquad \pi_m = \lambda_m . \int_0^r t . e^{-t.\lambda_m} dt$$

$$\pi_s = \lambda_s . \int_0^r t . e^{-t.\lambda_s} dt$$

and the fractional contribution (Z_λ) of each component to the total time spent in the closed state:

$$Z_f = \frac{\frac{a_f}{\lambda_f}}{\frac{a_f}{\lambda_f} + \frac{a_m}{\lambda_m} + \frac{a_s}{\lambda_s}} \qquad Z_m = \frac{\frac{a_m}{\lambda_m}}{\frac{a_f}{\lambda_f} + \frac{a_m}{\lambda_m} + \frac{a_s}{\lambda_s}}$$

$$Z_s = \frac{\frac{a_s}{\lambda_s}}{\frac{a_f}{\lambda_f} + \frac{a_m}{\lambda_m} + \frac{a_s}{\lambda_s}}. \tag{A4}$$

The unresolved occupancy of the "C" closed states is then given by:

$$E_{Cu} = E_C(\pi_f . Z_f + \pi_m . Z_m + \pi_s . Z_s).$$

From these equilibrium occupancy functions we can calculate the ratio τ_u/τ_i:

$$\frac{\tau_u}{\tau_i} = \frac{E_{Cu} + E_{Bu}}{E_O}$$

At 100 μM ACh, this expression yields values of τ_u/τ_i of 0.027 at −70 mV, 0.048 at −110 mV, and 0.054 at −150 mV. These values are, as expected, independent of tacrine concentration.

Since:

$$\tau_{app} = \tau_i + \tau_u = \tau_i\left(1 + \frac{\tau_u}{\tau_i}\right),$$

then from Eq. A2:

$$\tau_{app} = \frac{1 + \frac{\tau_u}{\tau_i}}{\alpha_a + [A].k_{Ba} + T.k_{T+1}}. \tag{A5}$$

From Eq. A5 it follows that:

$$\frac{1}{\tau_{app}} = \frac{a_a + A.k_{Ba} + T.k_{T+1}}{1 + \frac{\tau_u}{\tau_i}}. \tag{A6}$$

Substituting our calculated values of τ_u/τ_i into Eq. A6 reveals that using Eq. A3 with our data generates a maximum error of 5% in k_{T+1}. Thus, the calculations presented in this appendix demonstrate that correction of open times for missed gating and block events is unnecessary with our present data, and that plots of reciprocal apparent open time against tacrine concentration provide accurate estimates of k_{T+1}.

APPENDIX B

In Fig. 8, we plot the predicted rate constants and relative areas of the closed-time components arising from channel block. Below, we provide a derivation of the equations used to calculate these parameters.

In Scheme G2, states A_2B_T and A_2B_{TT} are connected to each other but not to any further closed states. The rate constants and relative areas of the exponentials corresponding to dwells in these two states can therefore be described using the following simplified scheme (state and rate constant definitions are as defined for Scheme G2 in the legend to Fig. 3).

$$A_2O \underset{k_{T-1}}{\overset{k_{T+1}.T}{\rightleftharpoons}} A_2B_T \underset{k_{T-2}}{\overset{k_{T+2}.T}{\rightleftharpoons}} A_2B_{TT}$$

3 1 2 (state number)

(SCHEME I)

Scheme I predicts a double exponential closed-time distribution with a p.d.f. of the form:

$$f(t) = a_1.\lambda_1 e^{-\lambda_1 t} + a_2.\lambda_2 e^{-\lambda_2 t},$$

where λ_1 and λ_2 are the rate constants of the two exponential components and a_1 and a_2 are the relative areas under the p.d.f. accounted for by λ_1 and λ_2. Note that a_1 and a_2 predict the areas of the exponentials corresponding to open channel block relative to each other in Scheme G2 but do not give information about the areas of these components relative to those of other closed states.

The transition rate matrix for Scheme I is:

$$Q = \begin{array}{c} \\ 1 \\ 2 \\ 3 \end{array} \begin{array}{c} \begin{array}{ccc} 1 & 2 & 3 \end{array} \\ \begin{bmatrix} -(k_{T-1} + k_{T+2}.T) & k_{T+2}.T & k_{T-1} \\ k_{T-2} & -k_{T-2} & 0 \\ T.k_{T+1} & 0 & -T.k_{T+1} \end{bmatrix} \end{array}$$

[1] In theory, the p.d.f for Scheme G2 should have four exponential components that arise from "C" closed states. The additional component is due to the closed blocked state. However, the closed blocked state has very low equilibrium occupancy and the rate constants connecting it to A_2C are slow compared with k_{-2} and β. Thus, the three component model used here should be a good approximation of reality.

Defining state A as the compound closed state and state B as the open state, the appropriate partition of Q is:

$$Q = \begin{bmatrix} Q_{AA} & Q_{AB} \\ Q_{BA} & Q_{BB} \end{bmatrix} = \left[\begin{array}{cc:c} -(k_{T-1} + k_{T+2.}T) & k_{T+2.}T & k_{T-1} \\ k_{T-2} & -k_{T-2} & 0 \\ \hdashline T.k_{T+1} & 0 & -T.k_{T+1} \end{array}\right]$$

Following the method of Colquhoun and Hawkes (1981), the Laplace transform of the p.d.f. of the closed time distribution is:

$$f_{13}^{*} = \frac{k_{T-1.}(s + k_{T-2})}{(s + \lambda_1)(s + \lambda_2)}. \tag{A7}$$

Inversion of Eq. A7 yields the required p.d.f.:

$$f_{13} = \frac{k_{T-1}(k_{T-2} - \lambda_1).\lambda_1.e^{-\lambda_1.t}}{\lambda_1(\lambda_2 - \lambda_1)} + \frac{k_{T-1}(\lambda_2 - k_{T-2}).\lambda_2.e^{-\lambda_2.t}}{\lambda_2(\lambda_2 - \lambda_1)} \tag{A8}$$

$$= a_1.\lambda_1 e^{-\lambda_1 t} + a_2.\lambda_2 e^{-\lambda_2 t}. \tag{A9}$$

The two rate constants λ_1 and λ_2 can then be found by solving the quadratic equation,

$$a\lambda^2 + b\lambda + c = 0,$$

where

$$a = 1$$
$$-b = \lambda_1 + \lambda_2 = k_{T-1} + k_{T-2} + k_{T+2.}T$$
$$c = \lambda_1.\lambda_2 = k_{T-1}.k_{T-2}$$

Using the familiar solution:

$$\lambda_1, \lambda_2 = \frac{-b \pm \sqrt{b^2 - 4ac}}{2a}$$

$$\lambda_1 = \frac{k_{T-1} + k_{T-2} + k_{T+2.}T + \sqrt{(k_{T-1} + k_{T-2} + k_{T+2.}T)^2 - 4k_{T-1}.k_{T-2}}}{2} \tag{A10}$$

$$\lambda_2 = \frac{k_{T-1} + k_{T-2} + k_{T+2.}T - \sqrt{(k_{T-1} + k_{T-2} + k_{T+2.}T)^2 - 4k_{T-1}.k_{T-2}}}{2} \tag{A11}$$

As expected, the rate constants and weights of the exponential components making up the block closed-time p.d.f. do not relate directly to individual states or transitions with the kinetic mechanism, so it is difficult to make intuitive predictions about how the closed-time distribution will vary with tacrine concentration. However, insight into the kinetics described by this model can be gained by examining its behavior under conditions of limiting low and high concentrations of tacrine.

Low Tacrine Concentration

At limiting low concentrations of tacrine, Eqs. A10 and A11 give:

$$\lambda_1 \approx k_{T-1} \quad \text{and} \quad \lambda_2 \approx k_{T-2}.$$

From Eqs. A8 and A9:

$$a_1 = \frac{k_{T-1}(k_{T-2} - \lambda_1)}{\lambda_1(\lambda_2 - \lambda_1)} \qquad a_2 = \frac{k_{T-1}(\lambda_2 - k_{T-2})}{\lambda_2(\lambda_2 - \lambda_1)}$$
$$\text{and} \quad a_1 + a_2 = 1. \tag{A12}$$

Substituting values of $\lambda_1 = k_{T-1}$ and $\lambda_2 = k_{T-2}$ into Eq. A12 yields $a_1 = 1$ and $a_2 = 0$. Thus, at very low concentrations of agonist, tacrine interacts solely with one binding site and Scheme G2 is indistinguishable from Scheme B1, the simple sequential mechanism for channel block.

High Tacrine Concentration

At high concentrations of tacrine, $b^2 \gg 4ac$ and $k_{T+1}.T \gg k_{T-1} + k_{T-2}$. Thus, from Eq. A10 we can approximate the faster rate constant, λ_1:

$$\lambda_1 \approx -b \approx T.k_T. \tag{A13}$$

The behavior of the slower rate constant, λ_2, is more conveniently examined using an alternative solution to the quadratic equation:

$$\lambda_1, \lambda_2 = \frac{2c}{-b \pm \sqrt{b^2 - 4ac}}. \tag{A14}$$

Again assuming that $b^2 \gg 4ac$ and $k_{T+1}.T \gg k_{T-1} + k_{T-2}$, Eq. A14 yields the following approximation for λ_2:

$$\lambda_2 \approx \frac{-c}{b} \approx \frac{k_{T-1}.k_{T-2}}{k_{T+2.}T}. \tag{A15}$$

The assumptions set out above also allow us to examine the behavior of the relative areas, a_1 and a_2, of the two p.d.f. components. From Eqs. A13 and A15, $\lambda_1 \gg \lambda_2$. Combining this with Eq. A12 therefore yields:

$$a_1 \approx \frac{k_{T-1}}{\lambda_1} \approx \frac{k_{T-1}}{T.k_{T+1}} \qquad \text{and} \qquad a_2 \approx 1 - \frac{k_{T-1}}{T.k_{T+1}}.$$

Thus, at high concentrations of tacrine, the mean duration and relative area of the exponential component governed by λ_1 and a_1 will both be inversely proportional to tacrine concentration. Conversely, there will be a linear relationship between the mean duration of the component of block closings governed by λ_2 and a_2

and tacrine concentration and the area of this component relative to a_1 will tend toward unity.

This work was supported by a grant from the Biotechnology and Biological Sciences Research Council (UK) to R.J. Prince and by NIH grant NS31744 to S.M. Sine.

Submitted: 28 February 2002
Revised: 8 July 2002
Accepted: 9 July 2002

REFERENCES

Adams, P.R. 1977. Voltage jump analysis of procaine action at frog end-plate. *J. Physiol.* 268:291–318.

Adams, P.R., and A. Feltz. 1980. End-plate channel opening and the kinetics of quinacrine (mepacrine) block. *J. Physiol.* 306:283–306.

Akaike, H. 1974. A new look at the statistical model identification. *IEEE Trans. Automatic Control.* AC-19:716–723.

Arias, H.R. 1996. Luminal and non-luminal non-competitive inhibitor binding sites on the nicotinic acetylcholine receptor. *Mol. Membr. Biol.* 13:1–17.

Auerbach, A., and G. Akk. 1998. Desensitization of mouse nicotinic acetylcholine receptor channels. A two-gate mechanism. *J. Gen. Physiol.* 112:181–197.

Auerbach, A., W. Sigurdson, J. Chen, and G. Akk. 1996. Voltage dependence of mouse acetylcholine receptor gating: different charge movements in di-, mono- and unliganded receptors. *J. Physiol.* 494:155–170.

Benoit, P., and J.P. Changeux. 1993. Voltage dependencies of the effects of chlorpromazine on the nicotinic receptor channel from mouse muscle cell line So18. *Neurosci. Lett.* 160:81–84.

Brejc, K., W.J. Van Dijk, R.V. Klaassen, M. Schuurmans, J. van Der Oost, A.B. Smit, and T.K. Sixma. 2001. Crystal structure of an ACh-binding protein reveals the ligand-binding domain of nicotinic receptors. *Nature.* 411:269–276.

Canti, C., E. Bodas, J. Marsal, and C. Solsona. 1998. Tacrine and physostigmine block nicotinic receptors in Xenopus oocytes injected with Torpedo electroplaque membranes. *Eur. J. Pharmacol.* 363:197–202.

Changeux, J.P. 1990. Functional architecture and dynamics of the nicotinic acetylcholine receptor, an allosteric ligand-gated ion channel. *Fida Research Foundation. Neuroscience Award Lectures.* 4:21–168.

Charnet, P., C. Labarca, R.J. Leonard, N.J. Vogelaar, L. Czyzyk, A. Gouin, N. Davidson, and H.A. Lester. 1990. An open-channel blocker interacts with adjacent turns of alpha-helices in the nicotinic acetylcholine receptor. *Neuron.* 4:87–95.

Clapham, D.E., and E. Neher. 1984. Substance P reduces acetylcholine-induced currens in isolated bovine chromaffin cells. *J. Physiol.* 347:255–277.

Clay, J.R., and L.J. DeFelice. 1983. Relationship between membrane excitability and single channel open-close kinetics. *Biophys. J.* 42: 151–157.

Colquhoun, D., and A.G. Hawkes. 1981. On the stochastic properties of single ion channels. *Proc. R. Soc. Lond. B Biol. Sci.* 211:205–235.

Colquhoun, D., and A.G. Hawkes. 1995. The principles of the stochastic interpretation of ion-channel mechanisms. *In* Single-Channel Recording. 2nd ed. B. Sakmann and E. Neher, editors. Plenum Press, New York. 397–482.

Colquhoun, D., and B. Sakmann. 1985. Fast events in single-channel currents activated by acetylcholine and its analogues at the frog muscle end-plate. *J. Physiol.* 369:501–557.

Dilger, J.P., R. Boguslavsky, M. Barann, T. Katz, and A.M. Vidal. 1997. Mechanisms of barbiturate inhibition of acetylcholine receptor channels. *J. Gen. Physiol.* 109:401–414.

Dilger, J.P., and Y. Liu. 1992. Desensitization of acetylcholine receptors in BC3H-1 cells. *Pflügers Arch.* 420:479–485.

Dolezal, V., V. Lisa, and S. Tucek. 1997. Effect of tacrine on intracellular calcium in cholinergic SN56 neuronal cells. *Brain Res.* 769: 219–224.

Dreixler, J.C., J. Bian, Y. Cao, M.T. Roberts, J.D. Roizen, and K.M. Houamed. 2000. Block of rat brain recombinant SK channels by tricyclic antidepressants and related compounds. *Eur. J. Pharmacol.* 401:1–7.

Evans, A.M., and R.J. Martin. 1996. Activation and cooperative multi-ion block of single nicotinic-acetylcholine channel currents of Ascaris muscle by the tetrahydropyrimidine anthelmintic, morantel. *Br. J. Pharmacol.* 118:1127–1140.

Franke, C., H. Hatt, H. Parnas, and J. Dudel. 1992. Recovery from the rapid desensitization of nicotinic acetylcholine receptor channels on mouse muscle. *Neurosci. Lett.* 140:169–172.

Hershkowitz, N., and M.A. Rogawski. 1991. Tetrahydroaminoacridine block of N-methyl-D-aspartate-activated cation channels in cultured hippocampal neurons. *Mol. Pharmacol.* 39:592–598.

Hunter, A.J., T.K. Murray, J.A. Jones, A.J. Cross, and A.R. Green. 1989. The cholinergic pharmacology of tetrahydroaminoacridine in vivo and in vitro. *Br. J. Pharmacol.* 98:79–86.

Jahn, K., B. Mohammadi, K. Krampf, A. Abicht, H. Lochmuller, and J. Bufler. 2001. Deactivation and desensitization of mouse embryonic- and adult-type nicotinic receptor channel currents. *Neurosci. Lett.* 307:89–92.

Katz, B., and S. Thesleff. 1957. A study of the desensitization produced by acetylcholine at the motor end-plate. *J. Physiol.* 138:63–80.

Kiefer-Day, J.S., H.E. Campbell, J. Towles, and E.E. el Fakahany. 1991. Muscarinic subtype selectivity of tetrahydroaminoacridine: possible relationship to its capricious efficacy. *Eur. J. Pharmacol.* 203:421–423.

Kojima, J., and K. Onodera. 1998. Effects of NIK-247 and tacrine on muscarinic receptor subtypes in rats. *Gen. Pharmacol.* 30:537–541.

Maconochie, D.J., and J.H. Steinbach. 1995. Block by acetylcholine of mouse muscle nicotinic receptors, stably expressed in fibroblasts. *J. Gen. Physiol.* 106:113–147.

Miller, C. 1989. Genetic manipulation of ion channels: a new approach to structure and mechanism. *Neuron.* 2:1195–1205.

Miyazawa, A., Y. Fujiyoshi, M. Stowell, and N. Unwin. 1999. Nicotinic acetylcholine receptor at 4.6 A resolution: transverse tunnels in the channel wall. *J. Mol. Biol.* 288:765–786.

Neely, A., and C.J. Lingle. 1986. Trapping of an open-channel blocker at the frog neuromuscular acetylcholine channel. *Biophys. J.* 50:981–986.

Neher, E. 1983. The charge carried by single-channel currents of rat cultured muscle cells in the presence of local anaesthetics. *J. Physiol.* 339:663–678.

Neher, E., and J.H. Steinbach. 1978. Local anaesthetics transiently block currents through single acetylcholine-receptor channels. *J. Physiol.* 277:153–176.

Ogden, D.C., and D. Colquhoun. 1985. Ion channel block by acetylcholine, carbachol and suberyldicholine at the frog neuromuscular junction. *Proc. R. Soc. Lond. B Biol. Sci.* 225:329–355.

Ohno, K., H.L. Wang, M. Milone, N. Bren, J.M. Brengman, S. Nakano, P. Quiram, J.N. Pruitt, S.M. Sine, and A.G. Engel. 1996. Congenital myasthenic syndrome caused by decreased agonist binding affinity due to a mutation in the acetylcholine receptor epsilon subunit. *Neuron.* 17:157–170.

Papke, R.L., and R.E. Oswald. 1989. Mechanisms of noncompetitive inhibition of acetylcholine-induced single-channel currents. *J. Gen. Physiol.* 93:785–811.

Pascual, J.M., and A. Karlin. 1998. Delimiting the binding site for quaternary ammonium lidocaine derivatives in the acetylcholine receptor channel. *J. Gen. Physiol.* 112:611–621.

Perry, E.K., C.J. Smith, J.A. Court, J.R. Bonham, M. Rodway, and J.R. Atack. 1988. Interaction of 9-amino-1,2,3,4-tetrahydroami-

noacridine (THA) with human cortical nicotinic and muscarinic receptor binding in vitro. *Neurosci. Lett.* 91:211–216.

Prince, R.J., and S.M. Sine. 1996. Molecular dissection of subunit interfaces in the acetylcholine receptor. Identification of residues that determine agonist selectivity. *J. Biol. Chem.* 271:25770–25777.

Prince, R.J., and S.M. Sine. 1998a. Epibatidine activates muscle acetylcholine receptors with unique site selectivity. *Biophys. J.* 75: 1817–1827.

Prince, R.J., and S.M. Sine. 1998b. Epibatidine binds with unique site and state selectivity to muscle nicotinic acetylcholine receptors. *J. Biol. Chem.* 273:7843–7849.

Qin, F., A. Auerbach, and F. Sachs. 1996. Estimating single-channel kinetic parameters from idealized patch-clamp data containing missed events. *Biophys. J.* 70:264–280.

Rao, C.R. 1973. Linear Statistical Inference and its Applications. Second Ed. John Wiley and Sons, Inc. New York.

Rayes, D., M.J. De Rosa, G. Spitzmaul, and C. Bouzat. 2001. The anthelmintic pyrantel acts as a low efficacious agonist and an open-channel blocker of mammalian acetylcholine receptors. *Neuropharmacology.* 41:238–245.

Sakmann, B., J. Patlak, and E. Neher. 1980. Single acetylcholine-activated channels show burst-kinetics in presence of desensitizing concentrations of agonist. *Nature.* 286:71–73.

Sine, S.M., T. Claudio, and F.J. Sigworth. 1990. Activation of *Torpedo* acetylcholine receptors expressed in mouse fibroblasts. Single channel current kinetics reveal distinct binding affinities. *J. Gen. Physiol.* 96:395–437.

Sine, S.M., and J.H. Steinbach. 1984. Agonists block currents through acetylcholine receptor channels. *Biophys. J.* 46:277–283.

Sine, S.M., and J.H. Steinbach. 1987. Activation of acetylcholine receptors on clonal BC3H-1 cells by high concentrations of agonist. *J. Physiol.* 385:325–359.

Sine, S.M., and P. Taylor. 1982. Local anesthetics and histrionicotoxin are allosteric inhibitors of the acetylcholine receptor. Studies of clonal muscle cells. *J. Biol. Chem.* 257:8106–8114.

Sine, S.M., H.-L. Wang, and N. Bren. 2002. Lysine scanning mutagenesis delineates structural model of the nicotinic receptor ligand binding domain. *J. Biol. Chem.* In press.

Spitzmaul, G., J.P. Dilger, and C. Bouzat. 2001. The noncompetitive inhibitor quinacrine modifies the desensitization kinetics of muscle acetylcholine receptors. *Mol. Pharmacol.* 60:235–243.

Svensson, A.L. 2000. Tacrine interacts with different sites on nicotinic receptor subtypes in SH-SY5Y neuroblastoma and M10 cells. *Behav. Brain Res.* 113:193–197.

Svensson, A.L., and A. Nordberg. 1996. Tacrine interacts with an allosteric activator site on alpha 4 beta 2 nAChRs in M10 cells. *Neuroreport.* 7:2201–2205.

Unwin, N. 1995. Acetylcholine receptor channel imaged in the open state. *Nature.* 373:37–43.

Vorobjev, V.S., and I.N. Sharonova. 1994. Tetrahydroaminoacridine blocks and prolongs NMDA receptor-mediated responses in a voltage-dependent manner. *Eur. J. Pharmacol.* 253:1–8.

Wilson, G.G., and A. Karlin. 1998. The location of the gate in the acetylcholine receptor channel. *Neuron.* 20:1269–1281.

Woodhull, A.M. 1973. Ionic blockage of sodium channels in nerve. *J. Gen. Physiol.* 61:687–708.

Zar, J.H. 1984. Biostatistical Analysis. Prentice-Hall, Inc., Englewood Cliffs, NJ. 718 pp.

Zhang, Y., J. Chen, and A. Auerbach. 1995. Activation of recombinant mouse acetylcholine receptors by acetylcholine, carbamylcholine and tetramethylammonium. *J. Physiol.* 486:189–206.

Zwart, R., R.G. van Kleef, C. Gotti, C.J. Smulders, and H.P. Vijverberg. 2000. Competitive potentiation of acetylcholine effects on neuronal nicotinic receptors by acetylcholinesterase-inhibiting drugs. *J. Neurochem.* 75:2492–2500.